Water Research 288 (2026) 124652

Contents lists available at ScienceDirect

Water Research

journal homepage: www.elsevier.com/locate/watres

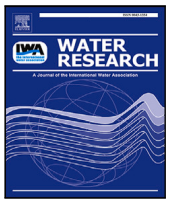

Transit times link pollution sources to drinking water quality in a "One Water" system

Shantanu V. Bhide [a,1], Stanley B. Grant [a,*,1], Paolo Benettin [b], Megan A. Rippy [a], Ahmed Monofy [a], Kirin E. Furst [a], Sydney Shelton [c], Sujay S. Kaushal [c], Shalini Misra [d], Peter J. Vikesland [e], Erin R. Hotchkiss [f], Anne Spiesman [g], Greg Prelewicz [g], Todd Schenk [h], Harold Post [a], Dongemei Alvi [a], Brian Steglitz [i], Admin Husic [a]

[a] Occoquan Watershed Monitoring Laboratory, Department of Civil and Environmental Engineering, Virginia Tech, 9408 Prince William St, Manassas, 20110, VA, USA
[b] Department of Earth Surface Dynamics, University of Lausanne, Quartier UNIL-Mouline, Lausanne, CH-1015, Switzerland
[c] Department of Geology, University of Maryland, Geology Bldg, 8000 Regents Dr, College Park, 20742, MD, USA
[d] School of Public and International Affairs, Virginia Tech, 900 N. Glebe Rd, Arlington, 22203, VA, USA
[e] Department of Civil and Environmental Engineering, Virginia Tech, 200 Patten Hall, Blacksburg, 24061, VA, USA
[f] Department of Biological Sciences, Virginia Tech, Blacksburg, 24061, VA, USA
[g] Fairfax Water, 8570 Executive Park Ave, Fairfax, 22031, VA, USA
[h] School of Public and International Affairs, Virginia Tech, 200 Stanger St., Blacksburg, 24061, VA, USA
[i] Upper Occoquan Service Authority, 14631 Compton Rd, Centreville, 20121, VA, USA

ARTICLE INFO

Keywords:
Unsteady transit time theory
Inland freshwater salinization
Reservoir water quality
One Water systems

ABSTRACT

Innovative approaches are needed to manage chronic and emerging water quality challenges in communities that rely on treated wastewater and urban stormwater as sources of raw water for drinking water treatment, or "One Water" systems. When amended to account explicitly for upstream versus distributed inflow to the reservoir, we show that unsteady transit time theory links pollution sources to water quality in the Occoquan Reservoir (Virginia, USA), one of the largest and oldest One Water systems in the United States. Using 11 years of hydrologic and water quality data, the model identified distinct sources and transformation rates for reactive (nitrate) and relatively non-reactive (sodium, chloride) solutes. High predictive skill was achieved with a strikingly small number of parameters: two for sodium and chloride (one for the upstream storage selection function, one for solute input from distributed sources; Nash–Sutcliffe Efficiency (NSE) = 0.65 and 0.76) and two additional for nitrate (capturing seasonal denitrification linked to summer stratification and hypolimnetic processes; NSE = 0.55). The simplicity of unsteady transit time theory supports rigorous parameter estimation (Bayesian Markov Chain Monte Carlo) and model structure evaluation (Bayesian Information Criterion). It also opens the door to real-time interactive simulations with stakeholders, supporting collaborative solutions to cascading water quality challenges.

1. Introduction

Historically, water systems have been managed as three distinct service components: drinking water, wastewater, and stormwater. Water practitioners worldwide are increasingly embracing integrated management of these systems to improve water quality, increase water supply reliability, reduce freshwater withdrawal, protect ecosystems, and achieve net energy and cost savings (Rahaman and Varis, 2005; Liu et al., 2020; Pokhrel et al., 2022; Grant et al., 2012). Widespread adoption of this One Water vision, as recommended by the Global Commission on the Economics of Water (Global Commission on the Economics of Water, 2024), requires moving beyond the siloed institutions that dominate today's practice (Mukheibir et al., 2014). In the United States, drinking water, wastewater, and stormwater are managed by separate organizations with different rules, norms, funding

* Corresponding author.
E-mail address: stanleyg@vt.edu (S.B. Grant).
[1] These authors contributed equally to this work.

https://doi.org/10.1016/j.watres.2025.124652
Received 2 July 2025; Received in revised form 24 August 2025; Accepted 20 September 2025
Available online 27 September 2025

models, and strategies (Pokhrel et al., 2022; Dombrowsky et al., 2022; Margerum, 2011; Crona and Parker, 2012; Kiparsky et al., 2016; Steel et al., 2017). This fragmentation poses barriers to the coordinated management of chronic and emerging water quality challenges, particularly for constituents such as sodium that lack clear regulatory remedies and therefore depend on voluntary, system-scale action by local actors (Ostrom, 2009; Rippy et al., 2024).

Predictability of system behavior and stakeholder understanding of system dynamics are key antecedents to the collaborative management of complex polycentric governance systems (Ostrom, 2009), including One Water systems (Grant et al., 2022). When dynamics are predictable, stakeholders can design more effective management strategies; when they are not, adaptive or precautionary approaches are often required (Nagel and Partelow, 2022). In this study, we examine how unsteady transit time theory can enhance predictability and deepen understanding of dynamic water quality patterns in One Water systems.

Unsteady transit time theory is a physics-based modeling approach that tracks the time-varying flux and age distribution of contaminants moving into and out of a control volume drawn around the system of interest (McGuire and McDonnell, 2006). As a lumped modeling approach, it avoids the need to resolve detailed internal hydraulics and transport processes (Lindenschmidt et al., 2019; Masoumi et al., 2016; Costa et al., 2021) and thus offers a simplified, data-driven alternative to conventional process-based models that can reduce computational demands, support rigorous model evaluation and parameter inference (Miles, 2019), and enable real-time deployment using data routinely collected by utilities.

Unsteady transit time theory has been widely applied in catchment hydrology to study water-age distributions, flow pathways, and solute transport (Benettin et al., 2022; McGuire and McDonnell, 2006; Hrachowitz et al., 2016; Rinaldo et al., 2011). It has also been used to model solute transport through transiently unsaturated soils (Kim et al., 2016), bioinfiltration systems (Parker et al., 2022), wetlands (Roa-García and Weiler, 2010), stream hyporheic zones (Harman et al., 2016), and alpine lakes (Smith et al., 2018). For many environmental applications a current limitation of unsteady transit time theory is the implicit assumption that all solutes and water share the same flow paths through the system of interest. This fundamental assumption breaks down when contaminants originate from spatially distinct sources with divergent hydrologic pathways (Liao et al., 2025).

To address this inherent limitation, we propose a dynamic mixing framework that partitions reservoir storage and outflow into separate contributions from upstream sources versus distributed shoreline sources. Combining this source-specific partitioning with unsteady transit time theory and solute-specific reaction models yields a tractable and generalizable modeling approach that preserves the strengths of age-based transport theory while explicitly accounting for the varied pollutant sources and flow pathways characteristic of One Water systems. This advance extends existing applications of unsteady transit time theory and provides a novel basis for real-time, source-resolved contaminant transport modeling in One Water systems and beyond.

We test this novel source-resolved version of unsteady transit time theory using data from the Occoquan Reservoir, a primary drinking water source for up to one million people in Northern Virginia (Fig. 1). The reservoir is among the first and largest examples of indirect potable reuse systems for surface water augmentation, the practice of deliberately adding advanced-treated wastewater, or "reclaimed water," to a drinking water reservoir (Randall and Grizzard, 1995). Reservoir inflows include reclaimed water from the Upper Occoquan Service Authority (UOSA) along with urban runoff and streamflow from the surrounding watershed (Bhide et al., 2021). UOSA employs a multi-barrier advanced treatment train that goes well beyond conventional secondary wastewater treatment, including biological nutrient removal, in which UOSA practices nitrification and seasonally adjusts denitrification to manage nitrate delivery to the reservoir, chemical phosphorus removal, media filtration, granular activated carbon, and disinfection. Fairfax Water's Griffith Drinking Water Treatment Plant draws its raw water from the downstream end of the reservoir near the Occoquan Dam. Water quality in the reservoir is managed by the drinking water utility (Fairfax Water), water reclamation facility (UOSA), and more than a dozen utilities and city, county, state, and federal government agencies (Grant et al., 2022).

For the past 50 years, these entities have navigated diverse water quality challenges through the Occoquan Policy (Virginia Administrative Code at 9 VAC 25-410), a state regulatory framework predating the U.S. federal Safe Drinking Water Act and Clean Water Act (Assembly, 1971). Today, the reservoir faces cascading water quality challenges spanning multiple regulatory contexts. These include nutrients such as nitrate and phosphorus, which have been regulated for decades (Randall and Grizzard, 1995); salts such as sodium and chloride, which are unregulated but have been increasing over time and could eventually affect finished water taste and contribute to excess dietary sodium intake (Kaushal et al., 2023); and newly regulated contaminants such as per- and polyfluoroalkyl substances (PFAS), two of which frequently exceed the U.S. EPA's recently promulgated maximum contaminant levels (MCLs) for drinking water at the Griffith intake (Environmental Protection Agency, 2024; Koban et al., 2024). Each pollutant class has various sources, including agricultural and urban runoff, contaminated groundwater, industrial discharges, and reclaimed water inputs.

The Occoquan Reservoir thus exemplifies the overlapping nutrient, salt, and emerging contaminant challenges that characterize modern One Water systems. In this first application of transit time theory to a reservoir, we focus on nitrate, sodium, and chloride for three reasons. First, these constituents are directly relevant to drinking water quality and have been monitored in the Occoquan at high frequency over multiple decades. Second, they originate from contrasting sources, follow distinct transport pathways, and display different seasonal dynamics, providing a rigorous test of the modeling framework. Finally, nitrate and chloride have long served as representative reactive and conservative tracers in watershed-scale transport studies (Kirchner et al., 2000; Benettin et al., 2015, 2022). Our results extends this end-member tracer framework to the reservoir scale, using nitrate, sodium, and chloride to probe the fate and transport of reactive (nitrate), conservative (chloride), and semi-conservative (sodium) constituents within a complex One Water system.

2. Theory

2.1. Conventional unsteady transit time theory

Application of unsteady transit time theory typically begins by performing a water budget over a control volume drawn around the system of interest, including inflows $J(t)$, outflows $Q(t)$, and storage $S(t)$ of water over time t (Fig. 2a and Table 1). Because water transports contaminants into and out of the control volume, the age distributions of water and contaminants in storage (residence time distribution) and outflow (transit time distribution) also vary with time. Here, the term "age" refers to the elapsed time between when a water parcel enters the reservoir (e.g., from an upstream tributary), $t_i > 0$, and some later time, $t \geq t_i$: $T = t - t_i$. Water and contaminants in reservoir storage and outflow have a range, or "distribution," of ages, reflecting the fact that they entered the reservoir at various times. For example, if $J(t)$ increases, the influx of new water (of age $T = 0$) will skew the age distributions of water and contaminants in storage and outflow toward younger values.

These age distributions are described mathematically by cumulative distribution functions (CDFs), $P_S(T,t)$ and $P_Q(T,t)$ (unitless), that represent the fraction of water in storage and outflow, respectively, with ages less than or equal to T at time t (Fig. 2b). The relationship between the unsteady hydrology of the system and water age distributions is defined by the Age Conservation Equation (ACE) (also referred

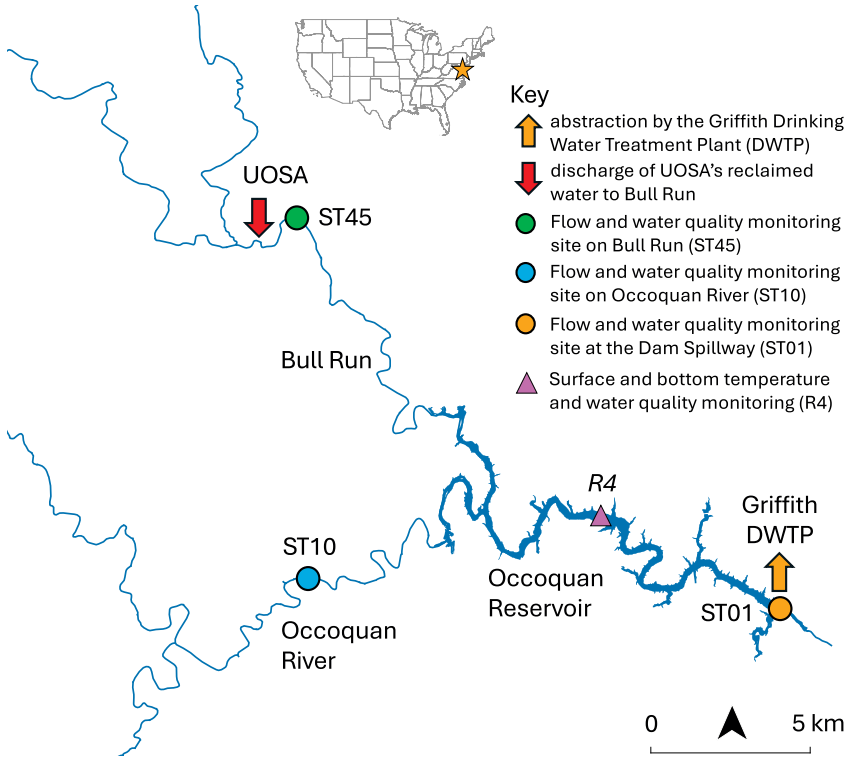

Fig. 1. The Occoquan Reservoir One Water system in Northern Virginia, U.S.A. Shown on the map are water quality and flow monitoring sites on the two major tributaries to the reservoir (Bull Run (ST45) and Occoquan River (ST10)) and at the base of the reservoir near the Occoquan Dam (ST01). Also shown are the discharge point where reclaimed water from the Upper Occoquan Service Authority (UOSA) enters Bull Run (red arrow), and the abstraction point where Fairfax Water's Griffith Drinking Water Treatment Plant (DWTP) intake is located (orange arrow). The pink triangle (R4) denotes the location on the reservoir where temperature and water quality are monitored at the surface and bottom of the reservoir on a weekly basis.

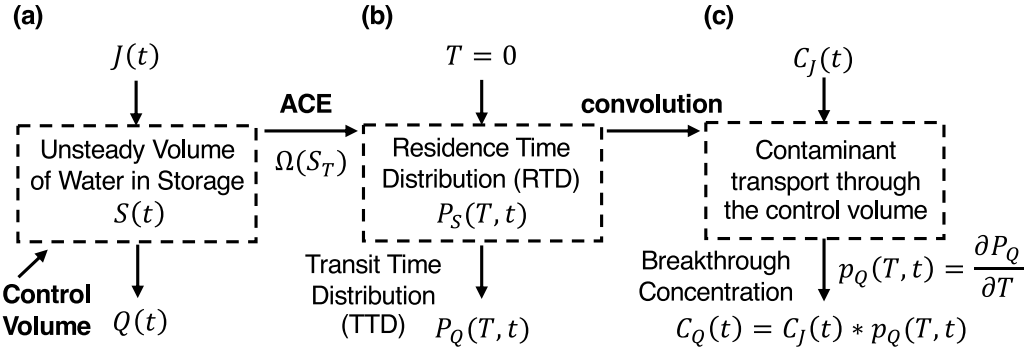

Fig. 2. Three steps in the conventional application of unsteady transit time theory. (**a**) A dynamic water balance is performed over a control volume enclosing the unsteady hydrologic or engineered system of interest, including inflows $J(t)$, outflows $Q(t)$, and water in storage $S(t)$. (**b**) The time varying age distributions of water in storage, $P_S(T,t)$, and outflow, $P_Q(T,t)$, are then calculated from the Age Conservation Equation (ACE, Eq. (1a)). This requires specifying a StorAge Selection (SAS) function, $\Omega(S_T)$, that indicates how the selection of water and solutes from storage for outflow is biased by age. (**c**) The breakthrough concentration of a contaminant leaving the control volume, $C_Q(t)$, is then computed by convolving the probability density function (PDF) form of the time-varying transit time distribution, $p_Q(T,t)$, with the time-varying concentration, $C_J(t)$, of contaminant entering the control volume (Eq. (2)).

to as the water age balance equation (Benettin et al., 2022)) shown schematically as the arrow between panels (a) and (b) of Fig. 2:

$$\frac{\partial S_T}{\partial t} = J(t) - Q(t)P_Q(T,t) - \frac{\partial S_T}{\partial T} \tag{1a}$$

$$S_T(T=0,t) = 0 \tag{1b}$$

$$S_T(T,t=0) = \begin{cases} 0, & T \le T_0 \\ S(t=0), & T > T_0 \end{cases} \tag{1c}$$

The ACE's dependent variable, age-ranked storage, $S_T(T,t)$ (units of volume), represents the volume of water in storage with age T or younger at time t. Mathematically, it is the product of the volume of water in storage and the water's residence time distribution: $S_T(T,t) = S(t) \times P_S(T,t)$. The ACE equates the time rate of change in age-ranked storage (left hand side Eq. (1a)) to the inflow of water of age $T = 0$ (first term right hand side), discharge of water from the control volume with transit time distribution $P_Q(T,t)$ (second term), and aging of water in storage (third term). The age boundary condition (Eq. (1b)) ensures

Table 1
List of variables, their descriptions, and dimensions.

Variable	Description	Dimensions
	Water balance variables	
$J(t), Q(t)$	daily reservoir inflows and outflows	[L^3 T^{-1}]
$S(t)$	daily reservoir storage	[L^3]
$J_{ST45}(t)$, $J_{ST10}(t)$, $J_{UOSA}(t)$	daily measured inflow at ST45, ST10, and UOSA	[L^3 T^{-1}]
$J_P(t)$	daily precipitation on reservoir	[L^3 T^{-1}]
$J_{OR}(t) = J_{ST10}(t)$	daily inflow from Occoquan River watershed	[L^3 T^{-1}]
$J_{BR}(t) = J_{ST45}(t) - J_{UOSA}(t)$	daily inflow from Bull Run watershed	[L^3 T^{-1}]
$J_{UG/GW}(t)$	daily inflow from ungauged surface water and groundwater	[L^3 T^{-1}]
$Q_{DWTP}(t)$, $Q_E(t)$, $Q_{Dam}(t)$	daily measured outflow from abstraction by the drinking water treatment plant (DWTP), evaporation off the reservoir surface, and discharge over the dam's spillway	[L^3 T^{-1}]
	Transit time variables	
t_i	time a water parcel enters the reservoir	[T]
t	time a water parcel is observed (e.g., in storage or outflow)	[T]
$T = t - t_i$	"age" of a water parcel in reservoir storage or outflow, $t \geq t_i$	[T]
$P_S(T,t)$, $P_Q(T,t)$	CDF form of age distributions in storage (residence time distribution, RTD) and outflow (transit time distribution, TTD)	[–]
$p_Q(T,t)$	PDF form of the TTD	[T^{-1}]
$S_T(t) = S(t)P_S(T,t)$	age-ranked storage	[L^3]
$\Omega(S_T,t)$	CDF form of the StorAge Selection (SAS) function	[–]
	Concentration variables	
$C_J(t)$, $C_Q(t)$	daily concentration in reservoir inflows and outflows	[M L^{-3}]
$C_{J,OR}(t)$, $C_{J,BR}(t)$, $C_{J,UOSA}(t)$, $C_{J,P}(t)$, $C_{J,UG/GW}(t)$	daily concentration in inflows from the Occoquan River, Bull Run, UOSA's reclaimed water, precipitation, and ungauged/groundwater sources	[M L^{-3}]
	Upstream vs Distributed source variables	
$f_2(t)$	fraction of storage from distributed sources	[–]
$J_1(t), Q_1(t)$	daily inflows and outflows from upstream sources	[L^3 T^{-1}]
$J_2(t), Q_2(t)$	daily inflows and outflows from distributed sources	[L^3 T^{-1}]
$S_1(t), S_2(t)$	daily storage from upstream and distributed sources	[L^3]
$\omega_1(t), \omega_2(t)$	fraction of outflow from upstream and distributed sources	[–]
$P_{S,1}(T,t)$, $P_{S,2}(T,t)$	CDF form of the RTD for upstream and distributed sources	[T^{-1}]
$p_{Q,1}(T,t)$, $p_{Q,2}(T,t)$	PDF form of the TTD for upstream and distributed sources	[T^{-1}]
$\Omega_1(T,t)$, $\Omega_2(T,t)$	SAS functions for upstream and distributed sources	[T^{-1}]
$C_{J,1}(t), C_{J,2}(t)$	inflow concentrations from upstream and distributed sources	[M L^{-3}]
$C_{Q,1}(t), C_{Q,2}(t)$	outflow concentrations from upstream and distributed sources	[M L^{-3}]
	Model fitting parameters	
a	coefficient for scaling $C_{J,OR}(t)$ to $C_{J,UG/GW}(t)$	[–]
p	Shifted-Uniform SAS parameter	[–]
α, β	Gamma SAS shape and scale parameters	[–] and [L^3]
k	stationary first-order rate constant	[T^{-1}]
c, d	coefficient and exponent for the non-stationary rate constant	[T^{-1}] and [–]

that no water in storage has age less than $T = 0$. The initial condition (Eq. (1c)) implies that all water in storage at time $t = 0$ has a single age, $T = T_0 \geq 0$. In practice, the solution to Eq. (1a) quickly loses memory of its initial condition.

If a single time-varying solute concentration, $C_J(t)$, can be assigned to all water flowing into the control volume, a major assumption underlying conventional unsteady transit time theory as noted earlier, then the "breakthrough concentration" of the solute leaving the control volume, $C_Q(t)$, can be calculated by filtering, or in mathematical terms convolving, the concentration of contaminant entering the control volume with the probability density function (PDF) form of the water's transit time distribution, $p_Q(T,t) = \frac{\partial P_Q(T,t)}{\partial T}$ (units of inverse age), shown schematically as an arrow between panels (b) and (c) in Fig. 2:

$$C_Q(t) = C_J(t) * p_Q(T,t) = \int_0^t C_J(t-T)p_Q(T,t)dT \tag{2}$$

Here, the symbol "$*$" denotes convolution. As we shall see, Eq. (2) can be amended to account for time-varying transit-time-dependent reaction of a contaminant as it passes through the control volume.

To solve Eq. (1a), a closure relationship is required to represent how the selection of contaminants from storage for outflow is biased by age (Kim et al., 2016):

$$P_Q(T,t) = \Omega(S_T,t) \tag{3}$$

The StorAge Selection (SAS) function, $\Omega(S_T,t)$ (unitless), is a CDF that represents the fraction of outflow drawn from each age-ranked volume-increment of water in storage (Kim et al., 2016). The SAS function is an emergent property of unsteady flow systems that captures: (1) the speed that water and solutes transit along flow paths through the control volume (advection); (2) where and when water and solutes enter the control volume, which determines the flow paths they transit along (source dispersion); and (3) local variation in flow velocities on adjacent flow paths (kinematic dispersion) (Hrachowitz et al., 2016). It is often assigned an analytical probability distribution, such as the Uniform, Plug-Flow, Gamma, or Beta (Hrachowitz et al., 2016; Harman, 2015; Grant and Harman, 2022; Kim et al., 2016). The SAS function can also vary with time, for example reflecting storage-dependent activation or deactivation of hydrologic flow paths through the control volume (Benettin et al., 2019; Kaandorp et al., 2018; Grant and Harman, 2022).

2.2. Extending unsteady transit time theory to upstream and distributed sources

Conventional unsteady transit time theory assumes that all water entering the control volume $J(t)$ can be assigned a single, time-varying contaminant concentration $C_J(t)$ (Fig. 2c). Here, we extend unsteady transit time theory to accommodate a key feature of pollutant loading in many environmental systems: inflowing water can originate from distinct sources with different time-varying contaminant concentrations. In the case of the Occoquan Reservoir, we postulate that pollutant loading to the reservoir can be roughly divided into two broad sources. One of these sources is the combined inflow from the Occoquan River and Bull Run at the head of the reservoir, including UOSA's reclaimed water; the other consists of groundwater and ungauged small tributaries that discharge to the reservoir along its perimeter. We refer to these as "upstream" and "distributed" sources, respectively, and denote them with subscripts 1 and 2 (see blue and orange inputs and flow paths in Fig. 3).

Given this conceptualization, the flow-weighted breakthrough concentration of a solute at the outlet, $C_Q(t)$, can be expressed as follows, where the variables $C_{Q,1}(t)$ and $C_{Q,2}(t)$ represent the outlet concentration of solute from upstream and distributed sources, respectively, and $\omega_1(t)$ and $\omega_2(t)$ are the corresponding fractions of total outflow, $Q(t)$ (Fig. 3c):

$$C_Q(t) = \omega_1(t)C_{Q,1}(t) + \omega_2(t)C_{Q,2}(t) \tag{4a}$$

$$\omega_1(t) = \frac{Q_1(t)}{Q(t)} \tag{4b}$$

$$\omega_2(t) = \frac{Q_2(t)}{Q(t)} \tag{4c}$$

$$Q(t) = Q_1(t) + Q_2(t) \tag{4d}$$

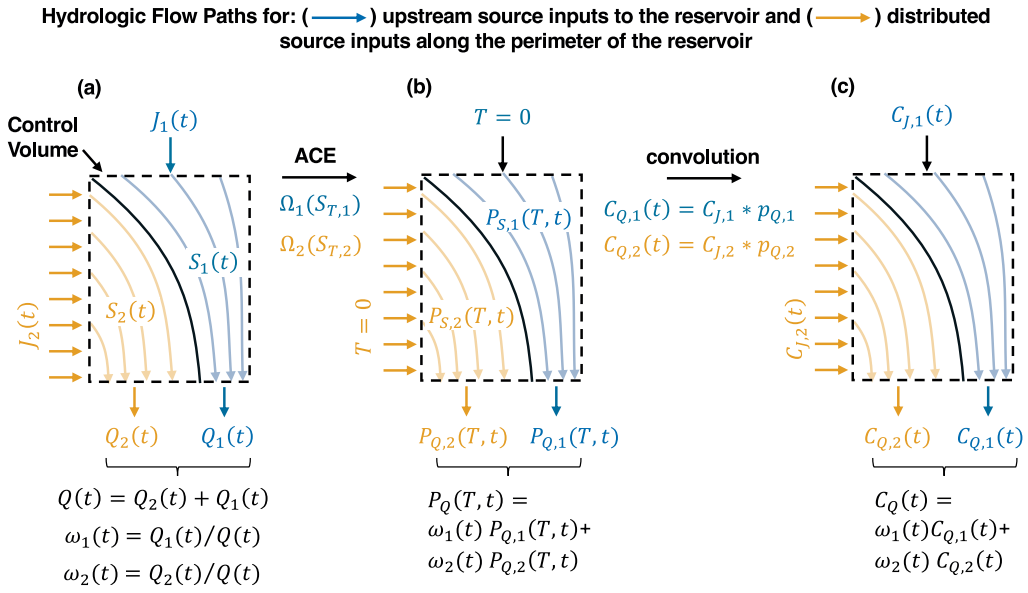

Fig. 3. Extension of unsteady transit time theory to include upstream and distributed pollutant and water sources (indicated here by the subscripts 1 and 2, respectively). (**a**) An unsteady water balance is performed separately for upstream and distributed sources, including inflows ($J_1(t), J_2(t)$), storage ($S_1(t), S_2(t)$), and outflows ($Q_1(t), Q_2(t)$). The total outflow is the sum of outflows originating from upstream and distributed sources (Eq. (4d)). (**b**) Once source-dependent SAS functions have been selected ($\Omega_1(S_{T,1}), \Omega_2(S_{T,2})$), the residence time distributions of upstream and distributed source water in storage ($P_{S,1}(T,t), P_{S,2}(T,t)$) and the transit time distributions of water in outflow ($P_{Q,1}(T,t), P_{Q,2}(T,t)$) can be calculated from the ACE (Eqs. (3) and (1a)). (**c**) The breakthrough concentration of a contaminant leaving the control volume, $C_Q(t)$, is the flow-weighted sum of outflow concentrations associated with upstream and distributed source inflows, obtained by convolving the source-dependent inflow concentrations and transit time distributions (Eqs. (5a) and (5b)).

The outflow concentrations $C_{Q,1}(t)$ and $C_{Q,2}(t)$ can be represented as convolutions of the inflow solute concentrations for these two sources ($C_{J,1}(t)$, $C_{J,2}(t)$) and their corresponding transit-time distributions ($p_{Q,1}(T,t)$, $p_{Q,2}(T,t)$) (arrow between panels (b) and (c), Fig. 3):

$$C_{Q,1}(t) = C_{J,1}(t) * p_{Q,1}(T,t) \tag{5a}$$

$$C_{Q,2}(t) = C_{J,2}(t) * p_{Q,2}(T,t) \tag{5b}$$

Combining Eqs. (4a)–(5b) we arrive at the following expression for the breakthrough concentration at the outlet:

$$C_Q(t) = \omega_1(t) \times \left(C_{J,1}(t) * p_{Q,1}(T,t)\right) + \omega_2(t) \times \left(C_{J,2}(t) * p_{Q,2}(T,t)\right) \tag{6}$$

2.3. Solving the water balance for upstream and distributed sources

To implement this extension of unsteady transit time theory, the ACE must be solved twice: once for upstream sources and once for distributed sources. This requires that the unsteady water balance over the control volume be known or estimated separately for each source (Fig. 3a). To that end, let $f_2(t) \in [0,1]$ [unitless] represent the fraction of total storage from distributed sources at any time t:

$$S_1(t) = (1 - f_2(t))S(t) \tag{7a}$$

$$S_2(t) = f_2(t)S(t) \tag{7b}$$

To proceed, we must make an assumption about how water from distributed sources in storage contributes to outflow. Given the broad spatial dispersion of distributed source inflows (orange arrows in Fig. 3), it is reasonable, at least as a starting point, to assume that this water is uniformly sampled for outflow across a wide distribution of travel times. These range from very short (e.g., for distributed source water entering near the base of the reservoir near the drinking water intake) to very long (e.g., for distributed source water entering at the far upstream end of the reservoir). Under this assumption, the fraction of distributed water in outflow matches its fraction in storage:

$$Q_1(t) = (1 - f_2(t))Q(t) \tag{8a}$$

$$Q_2(t) = f_2(t)Q(t) \tag{8b}$$

$$\omega_1(t) = (1 - f_2(t)) \tag{8c}$$

$$\omega_2(t) = f_2(t) \tag{8d}$$

Substituting Eqs. (7b) and (8b) into the dynamic water balance for distributed sources, $\frac{dS_2}{dt} = J_2(t) - Q_2(t)$, we arrive at the following differential equation for the fraction of water in storage and outflow from distributed sources:

$$\frac{df_2}{dt} = \frac{J_2(t)}{S(t)} - f_2(t)\frac{J(t)}{S(t)} \tag{9a}$$

$$f_2(0) = \frac{\bar{J}_2}{\bar{J}} \tag{9b}$$

The initial condition for $f_2(t)$ (Eq. (9b)) has been set equal to the average fraction of total inflow from distributed sources; the differential equation for $f_2(t)$ (Eq. (9a)) quickly loses memory of the initial condition (see Appendix A), so the choice of initial condition is somewhat arbitrary. In our application of Eq. (9a), the functions $S(t)$, $J(t)$ and $J_2(t)$ are known from measurements of pool elevation and inflow to the Occoquan Reservoir. Thus, Eq. (9a) can be solved numerically to yield $f_2(t)$, from which the complete dynamic water balance for upstream sources ($S_1(t)$ and $Q_1(t)$) and distributed sources ($S_2(t)$ and $Q_2(t)$) can be obtained (see Eqs. (7a)–(8b)).

3. Methods and materials

The extended version of unsteady transit time theory described above was applied to the Occoquan Reservoir on a daily timestep over an 11-year period, from January 1, 2010 to December 31, 2020, as follows.

3.1. Dynamic reservoir water balance

A daily reservoir water balance was performed over the 11-year period, including reservoir inflows, $J(t)$, reservoir outflows, $Q(t)$, and

reservoir storage, $S(t)$. Inflows to the reservoir include precipitation on the reservoir surface, $J_P(t)$, UOSA's reclaimed water, $J_{UOSA}(t)$, watershed runoff and urban runoff from Bull Run, $J_{BR}(t)$ and the Occoquan River, $J_{OR}(t)$, and net inputs from ungauged surface inflows and groundwater, $J_{UG/GW}(t)$. Outflows include evaporation off the reservoir surface, $Q_E(t)$, abstraction by the Griffith drinking water treatment plant, $Q_{DWTP}(t)$, and discharge over the dam's spillway, $Q_{Dam}(t)$.

$$\frac{dS}{dt} = J_P(t) + J_{UOSA}(t) + J_{BR}(t) + J_{OR}(t) + J_{UG/GW}(t) - Q_{DWTP}(t) - Q_E(t) - Q_{Dam}(t) \quad (10)$$

Daily storage volumes, $S(t)$, were estimated from measured reservoir pool elevation using a stage-volume rating curve. Stream and reclaimed water inflows were derived from gauged discharge measurements and utility data, while precipitation and evaporation were estimated from on-site weather observations. Outflow over the dam was estimated from a calibrated Weir equation (King, 1918), and net ungauged/groundwater inflow was estimated by difference. Additional details, including data sources and calibration procedures, are provided in Appendix B.

3.2. Dynamic upstream- and distributed-source water balance

Upstream-source inputs were defined, for the purposes of this study, to include water entering the head of the reservoir from Bull Run, UOSA's reclaimed water, and the Occoquan River:

$$J_1(t) = J_{BR}(t) + J_{UOSA}(t) + J_{OR}(t) \quad (11a)$$

$$J_{BR}(t) = J_{ST45}(t) - J_{UOSA}(t) \quad (11b)$$

$$J_{OR}(t) = J_{ST10}(t) \quad (11c)$$

Because UOSA's reclaimed water is discharged to Bull Run upstream of monitoring station ST45 (Fig. 1), the portion of flow coming from the Bull Run watershed can be isolated by taking the difference between the daily stream flow measured at ST45, $J_{ST45}(t)$, and the daily flow of UOSA's reclaimed water into Bull Run, $J_{UOSA}(t)$ (Eq. (11b)). The flow of water into the Occoquan Reservoir from the Occoquan River was equated to streamflow measurements at ST10, $J_{ST10}(t)$ (Eq. (11c)).

Distributed source inputs included precipitation on the reservoir surface and inflows along the perimeter of the reservoir from groundwater and smaller ungauged streams.

$$J_2(t) = J_P(t) + J_{UG/GW}(t) \quad (12)$$

While the inflow from direct precipitation on the reservoir was measured, inflow from small streams and groundwater along the reservoir's perimeter were inferred from all other measurements by rearranging Eq. (10).

From the daily estimates of distributed source inflows, $J_2(t)$, total inflow, $J(t) = J_1(t) + J_2(t)$, and reservoir storage, $S(t)$, the daily fraction of distributed source water in reservoir outflow, $f_2(t)$, was obtained by numerically integrating Eq. (9a). The corresponding proportion of reservoir outflow from upstream sources, $Q_1(t)$, and distributed sources, $Q_2(t)$, was computed from Eqs. (8a) and (8b), respectively, where the total daily outflow from the reservoir was estimated as follows:

$$Q(t) = Q_{DWTP}(t) + Q_E(t) + Q_{Dam}(t) \quad (13)$$

3.3. Inflow concentrations for upstream and distributed sources

During storm events, inflow to the Occoquan Reservoir can increase by several orders of magnitude, and in this region contaminant concentrations are often inversely correlated with flow (Bhide et al., 2021; Pandit et al., 2025). To obtain unbiased estimates of contaminant mass loading rates (Appling et al., 2015), we therefore constructed synthetic hourly time series of Na^+, Cl^-, and NO_3^- concentrations for all reservoir inflows based on daily-to-weekly measurements of these analytes in UOSA's reclaimed water and in grab samples collected at stations ST10 (upstream of the reservoir on the Occoquan River) and ST45 (upstream of the reservoir on Bull Run) (Fig. 1).

Specifically, multiple linear regression (MLR) models were created for each inflow and contaminant, adopting measured contaminant concentration as the dependent variable and a set of stakeholder-recommended environmental variables as potential covariates (Appendix C). Where data gaps prevented MLR model construction, a persistence model was adopted; i.e., daily concentrations were set equal to the last measured value (Heasley et al., 2021). These synthetic hourly concentration time series were paired with corresponding hourly flow data and aggregated into daily mass loads and average concentrations using the USGS software loadflex (Appling et al., 2015) for: (1) the Occoquan River, $C_{J,OR}(t)$, based on measurements on grab samples collected at ST10; (2) UOSA's reclaimed water, $C_{J,UOSA}(t)$, based on measurements on grab samples of the reclaimed water; and (3) Bull Run downstream of UOSA's discharge, based on measurements on grab samples collected at ST45, $C_{J,ST45}(t)$. The corresponding daily inflow concentration for Bull Run (upstream of UOSA's discharge point), $C_{J,BR}(t)$, was calculated by performing a daily mass balance over the confluence (see Appendix C for details).

Daily average contaminant concentrations in precipitation falling on the reservoir, $C_{J,P}(t)$, was estimated by adopting a persistence model on weekly National Atmospheric Deposition Program (NADP) data at station #MD99, the nearest NADP station, located approximately 50 km northeast of the reservoir in Beltsville, MD (Conrad-Rooney et al., 2023).

The daily average contaminant concentrations in ungauged streams and groundwater discharging to the reservoir are unknown, but are approximated here by using as a proxy concentrations measured in one of the other gauged inflows to the reservoir. There were three possible inflows that could have been used for this purpose: Occoquan River, $C_{J,OR}(t)$, Bull Run, $C_{J,BR}(t)$, or UOSA's reclaimed water, $C_{J,UOSA}(t)$. UOSA's reclaimed water was ruled out as treated sewage is unlikely to capture the magnitude or timing of inflow concentrations from ungauged streams and groundwater. Of the two gauged tributaries, the Occoquan River watershed is most similar to the ungauged portion of the watershed surrounding the reservoir in terms of land use and imperviousness. In 2016, the Occoquan River watershed was 5% impervious, 38% forested, and 18% developed, compared to 8% impervious, 53% forested, and 38% developed in the ungauged area. In contrast, the Bull Run watershed is more heavily developed (18% impervious, 30% forested, and 47% developed) (Dewitz, 2020). Therefore, concentrations in the inflow from ungauged and groundwater sources were approximated as follows, where a is model fitting parameter: $C_{J,UG/GW}(t) = aC_{J,OR}(t)$.

From the source-specific daily concentration estimates described above, we constructed daily timeseries of inflow concentrations from upstream sources, $C_{J,1}(t)$, and distributed sources, $C_{J,2}(t)$. The time-varying upstream concentration was calculated as the flow-weighted average of daily concentrations in UOSA's reclaimed water, $C_{J,UOSA}(t)$, along with watershed outflow from Bull Run, $C_{J,BR}(t)$, and the Occoquan River, $C_{J,OR}(t)$:

$$C_{J,1}(t) = \frac{C_{J,UOSA}(t)J_{UOSA}(t) + C_{J,BR}(t)J_{BR}(t) + C_{J,OR}(t)J_{OR}(t)}{J_{UOSA}(t) + J_{BR}(t) + J_{OR}(t)} \quad (14)$$

The time-varying distributed-source concentration was calculated as the flow-weighted average of daily contaminant concentrations in inflows from groundwater and ungauged streams along the reservoir's perimeter, $C_{UG/GW}(t)$, and direct precipitation on the reservoir, $C_P(t)$:

$$C_{J,2}(t) = \frac{C_{J,UG/GW}(t)J_{UG/GW}(t) + C_{J,P}(t)J_P(t)}{J_{UG/GW}(t) + J_P(t)} \quad (15)$$

3.4. StorAge selection (SAS) functions for upstream and distributed sources

3.4.1. SAS function for distributed sources

Consistent with the assumption underlying the water balance for distributed sources (see Eq. (9a) and discussion thereof), we assumed that a uniform SAS describes the selection of distributed source water and contaminants for outflow from the reservoir, $\Omega_2(S_T)$.

3.4.2. SAS functions for upstream sources

Five different candidate SAS functions were trialed for the selection of upstream source water and contaminants from storage for outflow from the reservoir, $\Omega_1(S_t)$, including the Shifted-Uniform, Uniform, Plug Flow, stationary Gamma, and non-stationary Gamma (Kim et al., 2016). The Shifted-Uniform function is a recently introduced stationary SAS function whose single parameter, $p \in [0,1]$, indicates where an unsteady hydrologic system falls along a spectrum between a pure Uniform SAS function ($p = 0$) and a pure Plug Flow SAS function ($p = 1$) (Grant and Harman, 2022). As recommended by Harman and Xu Fei (2024), both stationary and non-stationary versions of the Gamma distribution were evaluated. The stationary version has two parameters, a shape parameter α (unitless) and a scale parameter β (units of volume). The non-stationary version has only one parameter (the shape parameter, α) because the scale parameter is set equal to the measured volume of water in reservoir storage, $\beta(t) = S_1(t)$. Details are presented in Appendix B.

3.5. Kinetic models for in-reservoir contaminant removal

We evaluated three kinetic models of in-reservoir contaminant removal: null, stationary, and non-stationary.

3.5.1. No removal (null model)

The Null Model, evaluated for all three contaminants (Na^+, Cl^-, and NO_3^-), assumes that no removal occurs as water transits the reservoir.

3.5.2. Stationary first-order removal (stationary model)

The Stationary Model, which was evaluated for all three contaminants (Na^+, Cl^- and NO_3^-), assumes that in-reservoir removal follows transit-time dependent first-order kinetics with a fixed rate constant k (units of inverse residence time).

3.5.3. Non-stationary first-order removal (non-stationary model)

For NO_3^-, we also evaluated a non-stationary first-order rate model that accounts for seasonal and temperature-driven variability in the rate constant, $k(t)$. This was motivated by two key observations: (1) UOSA seasonally adjusts its denitrification processes to increase nitrate concentrations in reclaimed water during summer stratification, with the goal of limiting hypolimnetic anoxia and the associated release of phosphorus and heavy metals from reservoir sediments (Randall and Grizzard, 1995); and (2) much of the nitrate released by UOSA during this period is subsequently denitrified in the reservoir, as nitrate-rich effluent mixes into the oxygen-depleted hypolimnion. To capture this seasonal variability in the reservoir's denitrification capacity (which is greater during stratification), we allowed the removal rate constant $k(t)$ to vary with surface water temperature (Palacin-Lizarbe et al., 2018) where Temp(t) is weekly measured reservoir surface water temperature at station R4 (pink triangle, Fig. 1), Temp_{avg} is the 11-year average of surface water temperature measured at station R4, and c and d are model fitting parameters:

$$k(t) = c\left(\frac{\text{Temp}(t)}{\text{Temp}_{\text{avg}}}\right)^{d} \tag{16}$$

3.5.4. Incorporating removal into the convolution integrals

The null (NULL), stationary (S) and non-stationary (NS) kinetic models described above for contaminant removal in the reservoir were incorporated into the convolution integrals in Eq. (6) as follows:

$$(C_J * p_Q)^{\text{NULL}} = \int_0^t C_J(t-T)\, p_Q(T,t)\, dT \tag{17a}$$

$$(C_J * p_Q)^{\text{S}} = \int_0^t C_J(t-T)\, p_Q(T,t)\, e^{-kT}\, dT \tag{17b}$$

$$(C_J * p_Q)^{\text{NS}} = \int_0^t C_J(t-T)\, p_Q(T,t)\, e^{-\int_{t-T}^{t} k(x)\,dx}\, dT \tag{17c}$$

3.6. Parameter inference and model structure ranking

Model calibration and model structure selection proceeded in two steps. First, the model was fit to 11 years of weekly or higher frequency Na^+ and Cl^- measurements at the base of the reservoir near the drinking water intake (station ST01, yellow star in Fig. 1). The goal of this first step was to identify an appropriate SAS function for upstream sources of water and contaminants (i.e., contaminants entering the reservoir from UOSA's reclaimed water, the Occoquan River, and Bull Run, $\Omega_1(S_t)$), using a set of analytes (sodium and chloride) which, as will be documented below, behave relatively conservatively as they transit through the reservoir. To this end, a total of 10 different model structures were evaluated for Na^+ and Cl^- (Tables E.1 and E.2), including combinations of five SAS functions (Shifted-Uniform, Uniform, Plug Flow, stationary Gamma, and non-stationary Gamma) and two kinetic models (Null and Stationary first-order removal).

The upstream-source SAS function, $\Omega_1(S_t)$, identified in the first step should apply equally well to any contaminant entering the reservoir from reclaimed water and the upstream tributaries. Accordingly, in the second step the best-performing SAS function from the first step was used to model the transport of NO_3^- under a broader set of removal assumptions (Null, Stationary, and Non-Stationary). The focus of this second step was to calibrate the Non-Stationary model for nitrate removal in the reservoir, and compare its performance to the Null and Stationary kinetic models.

Model fitting was carried out using Bayesian Markov Chain Monte Carlo (MCMC) simulations implemented in the *pymcmcstat* Python package (Miles, 2019). The model fitting exercise excluded the first 120-days of the 11-year study period, to allow for model spin-up (see Appendix A). The number of inferred parameters ranged from one (for the Uniform or Plug Flow SAS functions paired with the Null kinetic model) to five (for the stationary Gamma SAS function paired with the Non-Stationary kinetic model; see Appendix E). All model simulations were performed using *mesas.py* (Harman and Xu Fei, 2024).

Model performance was evaluated with respect to both predictive error and model parsimony. Predictive error was quantified using the root mean squared error (RMSE) between simulated breakthrough concentrations and observed concentrations at the base of the reservoir near the drinking water intake (at station ST01, Fig. 1), as well as Nash–Sutcliffe Efficiency (NSE) which ranges from -∞ to 1, where negative values indicates that the model represents the data worse than the mean and the upper limit indicates a perfect representation of the data (Weglarczyk, 1998). The different model structures were ranked by Bayesian Information Criterion (BIC), which penalizes overparameterization (Brewer et al., 2016).

3.7. Field data collection and analytical methods

Na^+, Cl^-, and NO_3^- concentrations in reclaimed water were reported by UOSA and measured by a certified in-house or commercial laboratory using standard methods. All other measurements of these three analytes were performed by the Occoquan Watershed Monitoring Laboratory (OWML) in Manassas, Virginia, using standard methods. Weekly grab samples collected from the dam spillway (ST01), downstream of

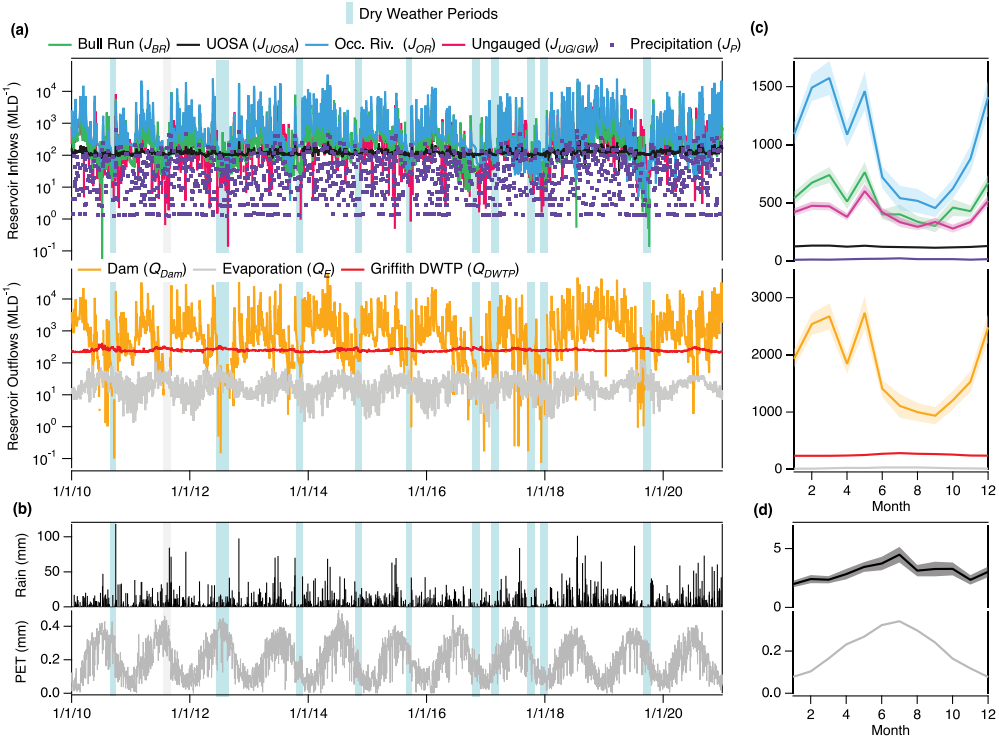

Fig. 4. **(a)** Daily inflows (top panel) and outflows (bottom panel) for the Occoquan reservoir over 11 years, from January 1 2010 to December 31, 2020 ($N = 4018$ days). Vertical light blue stripes denote dry weather periods when inflows from the watershed fall near or below inflow from UOSA's reclaimed water. **(b)** Daily rainfall (top panel) and NASA Land Surface Model estimates of potential evapotranspiration (PET, bottom panel) in the watershed ($0.125° \times 0.125°$ pixel centered on the nearby Occoquan Forest). **(c)** Monthly average values of inflows and outflows. **(d)** Monthly average values of daily rainfall and PET estimates in (c). Shaded bands represent standard error of the mean. Numbered months in panels (c) and (d) are as follows: 1 = January; 2 = February; 3 = March; 4 = April; 5 = May; 6 = June; 7 = July; 8 = August; 9 = September; 10 = October; 11 = November; 12 = December.

UOSA on Bull Run (ST45), and from the Occoquan River (ST10) were field-filtered using 0.45 μm syringe filters (Filtrous Lab, 30 mm GFP) and transported on ice to the OWML within 4 h of collection. Within 24 h of arrival, the pre-filtered samples were analyzed for Na^+, Cl^- using ion chromatography (Dionex ICS-5000), following ASTM D6919-09 and Standard Method 4110 B-2011. At the same sampling sites, additional (unfiltered) samples were collected and transported to the OWML on ice where they were immediately filtered through a 1.5 μm glass microfiber filter (Whatman, 934-AH) and stored at −20 °C prior to analysis. Within 28 days of arrival, 200 mL of the filtered sample was analyzed for dissolved nitrate (Astoria Pacific, Model 311 Autoanalyzer with 305D Detector; SM4500-NO_3^- F). Nitrate concentrations are reported as mg/L of N. All analyses were conducted in accordance with the OWML's Virginia Environmental Laboratory Accreditation Program (VELAP #460026).

Daily stream discharge at gauge stations on the Occoquan River (ST10) and on Bull Run (ST45), and flow out of the reservoir through the dam's spillway (ST01) were also measured by the OWML (Appendix B). Daily discharge of reclaimed water to Bull Run was provided by UOSA. Daily precipitation on the reservoir surface was measured at a rain gauge in Lorton, VA, near station ST01 (Appendix B). Daily estimates of local potential evapotranspiration (PET) in the watershed (for a pixel ($0.125° \times 0.125°$) centered on the nearby Occoquan Forest) were obtained from NASA's land surface model (NLDAS-Noah) using the Data Rods Explorer (https://apps.hydroshare.org/apps/data-rods-explorer).

4. Results

4.1. Reservoir water balance

Over the 11-year study period, average daily inflows to the reservoir, $J(t)$, decreased in order (top panel, Fig. 4a): Occoquan River (987 megaliters per day (ML day^{-1})) > Bull Run (520 ML day^{-1}) > ungauged sources (361 ML day^{-1}) > UOSA's reclaimed water (125 ML day^{-1}) > direct precipitation on the reservoir surface (17 ML day^{-1}). Average daily outflows from the reservoir decreased in order (bottom panel, Fig. 4a): flow over the Dam's spillway (1735 ML day^{-1}) > abstraction by Fairfax Water's Griffith Drinking Water Treatment Plant (253 ML day^{-1}) > evaporation (22 ML day^{-1}). Reservoir storage varied from 28 to 44 GL, with a mean of 33 GL.

On a day-to-day basis, inflow from the watersheds varies dramatically (in some cases increasing >100-fold during storm events) while inflow of UOSA's reclaimed water is relatively steady. Occasionally, during prolonged dry weather, inflow to the reservoir from Bull Run and the Occoquan River fall close to, or below, inflow from UOSA's reclaimed water, highlighting the drought resilience benefits of indirect potable reuse in this system (see vertical light blue stripes, Fig. 4a,b). During these dry weather periods the primary outflow from the reservoir is abstraction by the Griffith DWTP.

The corresponding seasonal patterns are illustrated in Figs. 4c,d. Despite higher average precipitation during the summer, monthly average inflow to the reservoir from the Occoquan River and Bull Run decline sharply from June through September (Fig. 4c), reflecting the influence of increased evapotranspiration across the watershed in the summer (Figs. 4d). The seasonal pattern of outflow from the reservoir over the dam spillway closely follows the seasonal patterns of inflow from the Occoquan River and Bull Run (compare top and bottom panels, Figs. 4c).

4.2. Upstream and distributed source water balance

The daily inflows described in the previous section were partitioned into upstream sources, $J_1(t)$, and distributed sources, $J_2(t)$ (see Eqs. (12) and (11a)). On average, upstream sources account for ≈ 78% of total

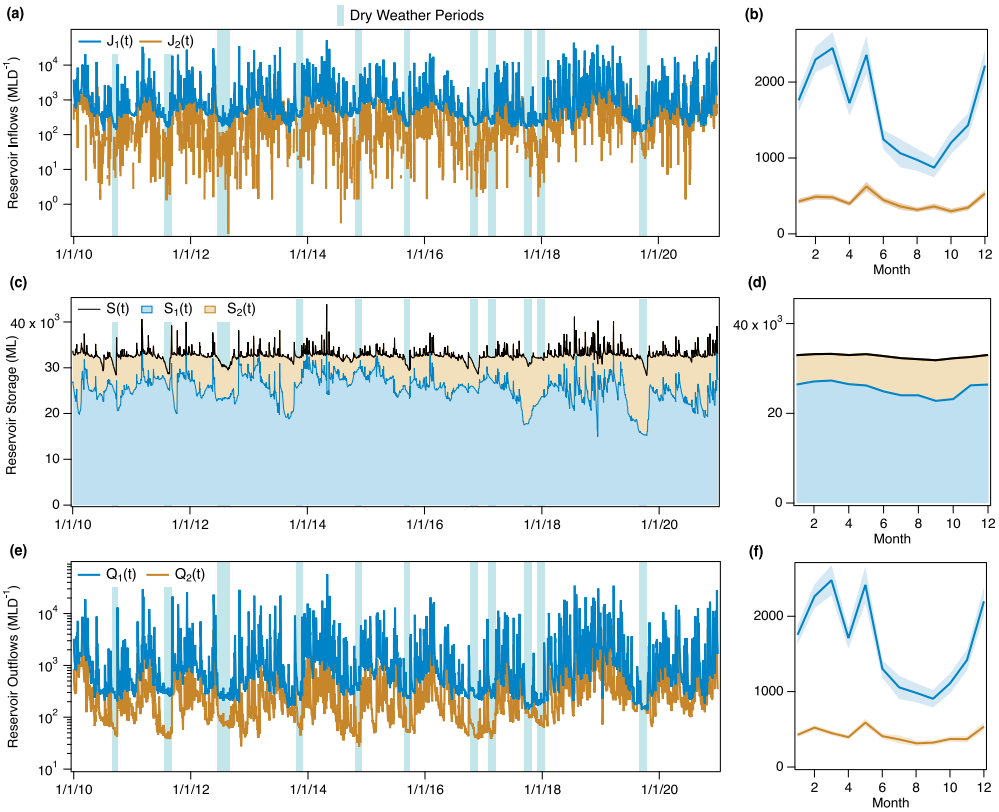

Fig. 5. Measured or imputed daily (left panels) and monthly average (right panels) inflows, storage, and outflows associated with upstream sources (Occoquan River, Bull Run, and UOSA's reclaimed water) and distributed sources (small ungauged streams and groundwater inflows along the reservoir's perimeter, along with direct wet deposition on the reservoir surface). Vertical light blue stripes denote dry weather periods when inflows from the watershed fall close to, or below, inflow from UOSA's reclaimed water. **(a, b)** Inflows from upstream, $J_1(t)$, and distributed, $J_2(t)$, sources. **(c, d)** Division of total reservoir storage volume between upstream, $S_1(t)$, and distributed, $S_2(t)$, sources. **(e, f)** Reservoir outflows from upstream, $Q_1(t)$, and distributed, $Q_2(t)$, sources. Shaded bands in panels (b), (d), and (f) represent standard error of the mean (not visible in some cases).

inflow to the reservoir, while distributed sources contribute ≈ 22%. Both exhibit substantial day-to-day variability, reflecting higher inflows during storm events (Fig. 5a). Seasonal variability is stronger in upstream inflows, which are higher in winter and lower in late summer, while distributed inflows are more constant over the year (Fig. 5b).

The daily fraction of reservoir storage originating from distributed sources, $f_2(t)$, was estimated by numerically integrating Eq. (9a). Over the 11-year study period, the fraction $f_2(t)$ ranged from 5 to 51%, with a mean (= 22 ± 10%) precisely equal to the fraction of inflow from distributed sources. The resulting partitioning of storage between upstream and distributed sources ($S_1(t)$ and $S_2(t)$; Eqs. (7a) and (7b)) shows both daily and seasonal variability. Storms temporarily increase contributions from both upstream and distributed sources (Fig. 5c), while the seasonal mix of water in storage shifts toward upstream sources in winter and toward distributed sources in late summer and early fall (Fig. 5d).

The seasonal cycles of upstream and distributed outflows closely track the seasonal cycles of upstream and distributed inflows, indicating that on a month-to-month basis inflows and outflows from each source are effectively balanced (Fig. 5b,f). On daily timescales, however, the most striking difference is in the minimum values: distributed inflows ($J_2(t)$) frequently decline to near zero during dry periods (vertical light blue stripes), whereas distributed outflows ($Q_2(t)$) remain sustained (compare brown curves in Figs. 5a and e). This pattern reflects the reservoir's buffering role: the release of previously stored water from distributed sources maintains a base level of outflow, effectively raising the minimum outflow during inflow deficits while preserving the broader seasonal cycle.

4.3. Upstream source pollutant concentrations

Fig. 6a shows daily measured or imputed values of Na^+, Cl^-, and NO_3^- concentrations in upstream source ($C_{J,1}$) inflows to the reservoir (blue points in the figure). Among the three upstream sources (reclaimed water, Bull Run, and the Occoquan River), concentrations in UOSA's reclaimed water ($C_{J,\mathrm{UOSA}}$) are generally highest, except during winter deicer wash-off events when Na^+ and Cl^- levels in Bull Run and the Occoquan River occasionally exceed those in reclaimed water (compare blue and black points in the top two panels of Fig. 6a).

Seasonal trends in upstream-source concentrations include (blue curves, Fig. 6b): (1) bimodal peaks in Na^+ and Cl^-, with winter peaks driven by deicer runoff from impervious urban areas in the Occoquan River and Bull Run watersheds and summer peaks likely reflecting reduced dilution of UOSA's effluent during periods of low inflow from those watersheds; and (2) a strong summer peak in NO_3^-, consistent with UOSA's seasonal practice of suspending denitrification treatment processes (and thereby increasing nitrate concentrations in their reclaimed water) to help reduce hypolimnetic anoxia and limit the release of phosphorus and heavy metals from bottom sediments when the reservoir is stratified in the summer (Randall and Grizzard, 1995).

4.4. Parameter inference and model performance

Given the reservoir water balance and inflow concentrations presented above, we next evaluated a suite of transit time models (each combining alternative upstream source SAS functions and kinetic removal models) for their ability to reproduce weekly measurements of Na^+, Cl^- and NO_3^- at the base of the reservoir near the Griffith DWTP

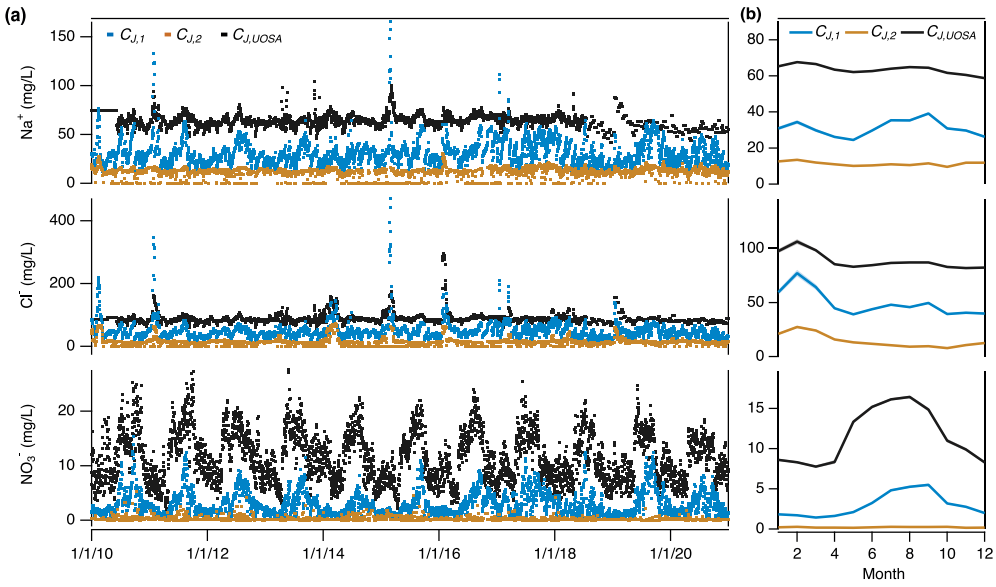

Fig. 6. Measured or imputed Na^+, Cl^-, and NO_3^- concentrations in reservoir inflows from upstream sources (Occoquan River, Bull Run, and reclaimed water) and distributed sources (surface and groundwater inflows along the perimeter of the reservoir, and wet deposition on the reservoir surface). Daily values (left panels) and corresponding monthly averages (right panels) are shown separately for upstream sources (blue points and lines) and distributed sources (brown points and lines). Reclaimed water is shown separately for comparison (black points and lines).

Table 2
Inferred mean [95% CI] parameter values for Na^+, Cl^- and NO_3^-.

Pollutant	a (unitless)	p (unitless)	c (units of inverse days)	d (unitless)	RMSE (units of mg/L)	NSE (unitless)
Na^+	0.97 [0.96, 0.98]	0.51 [0.51, 0.51]	–	–	4.79	0.65
Cl^-	0.63 [0.63, 0.64]	0.51 [0.51, 0.51]	–	–	6.86	0.76
NO_3^-	0.28 [0.05, 0.85]	–	7.4 [6, 10] $\times 10^{-3}$	29 [21, 36]	0.29	0.55

intake (station ST01, Fig. 1). Top-performing model variants were selected primarily based on parsimony (Bayesian Information Criterion, BIC) as summarized next.

4.4.1. Distributed source concentrations

One of the parameter values obtained through model fitting was the scaling constant, a, which converts measured concentrations in the Occoquan River into corresponding concentrations in ungauged surface water and groundwater entering the reservoir along its perimeter: $C_{UG/GW} = aC_{OR}$. In effect, the model uses concentrations measured in the Occoquan River as a proxy for concentrations in ungauged/groundwater inputs, with the parameter a adjusting the magnitude of this proxy to best match observed concentrations of Na^+, Cl^-, and NO_3^- at the base of the reservoir near the Griffith intake. The inferred values of a (Table 2) suggest that, on average, ungauged/groundwater concentrations are lower than Occoquan River concentrations (i.e., $a < 1$), which are already low compared to concentrations measured in Bull Run and UOSA's reclaimed water (Figure C.1). Because measured concentrations in rain are also quite low (Figure C.1), the resulting distributed source concentrations ($C_{J,2}(t)$, Eq. (15)), are substantially lower than upstream source concentrations ($C_{J,1}(t)$, Eq. (14)) and exhibit less seasonal variability (brown curves and points in Fig. 6a,b). An exception is Cl^-, which shows a modest wintertime increase, likely reflecting road salt and perhaps septic field inputs from low-density residential communities located in the portion of the watershed that drains to the reservoir's perimeter (as of 2016, 8% impervious).

4.4.2. SAS function for upstream-source water and solute transport

Five candidate SAS functions were evaluated for their ability to reproduce measured Na^+ and Cl^- concentrations at the base of the reservoir. For Cl^-, the Shifted-Uniform SAS had the lowest BIC (Table E.2). For Na^+, the stationary Gamma and Shifted-Uniform SAS functions have similar BIC values (1767 and 1773, respective, Table E.1). However, a strong correlation between the Gamma function's shape (α) and scale (β) parameters indicates an equifinality problem; i.e., multiple combinations of the Gamma function's parameter values yield similar model performance (Figure E.2). Accordingly, the Shifted-Uniform SAS was selected to represent upstream source transport through the reservoir. Inferred values of the Shifted Uniform's single parameter were the same for both solutes: $p = 0.51 \pm 0.003$ (Table 2 and Figure E.1.).

4.4.3. Kinetic models for Na^+, Cl^-, and NO_3^- removal

For Na^+ and Cl^-, the Null Model yielded the lowest BIC, indicating no appreciable removal as these ions pass through the reservoir (Tables E.1 and E.2). In contrast, the Non-Stationary Kinetic Model (Eq. (16)) performed best for NO_3^- (Table 2; Table E.3; Figure E.1), with most removal occurring during summer stratification (Fig. 7a). The corresponding annual average denitrification rate (4.9 ± 3.7 mol N m^{-2} $year^{-1}$) is at the high end of values previously reported for lakes and reservoirs (0.013–2.93 mol N m^{-2} $year^{-1}$) (Piña-Ochoa and Álvarez-Cobelas, 2006; Mulholland et al., 2008) (Fig. 7b) consistent with the highly managed nature of nitrate in this system. Specifically, as noted earlier, during periods of reservoir stratification UOSA suspends denitrification treatment processes, thereby increasing the nitrate concentrations in their reclaimed water (see black points, bottom panel, Fig. 6a). The resulting combination of high nitrate concentrations, low dissolved oxygen, and abundant organic carbon concentrations provide ideal conditions for hypolimnetic denitrification (Seitzinger et al., 2006).

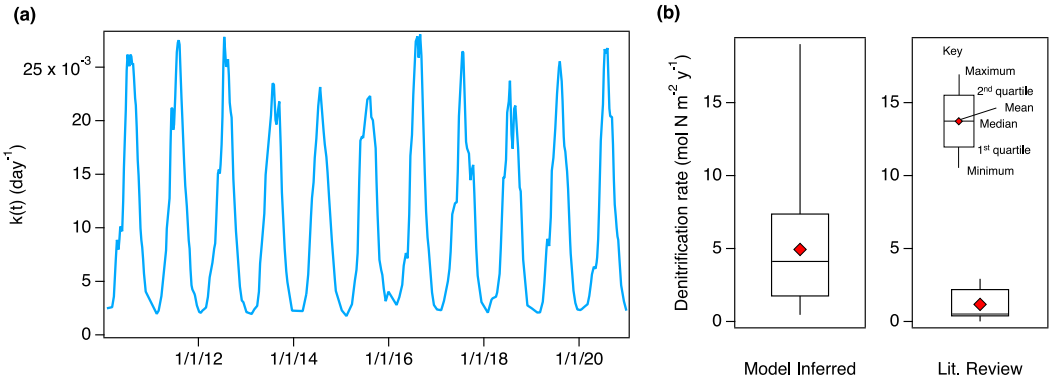

Fig. 7. **(a)** The model-inferred non-stationary first-order reaction rate constant for nitrate removal in the reservoir, $k(t)$. **(b)** Model-inferred in-reservoir denitrification rate compared to denitrification rates previously reported for lakes and reservoirs ($N = 30$) (Piña-Ochoa and Álvarez-Cobelas, 2006; Mulholland et al., 2008). The model-inferred denitrification rate was calculated from the non-stationary first-order rate constant as follows, $r(t) = k(t)C(t)h(t)$, where $C(t)$ and $h(t)$ are the average measured nitrate concentration and water depth in the reservoir, respectively.

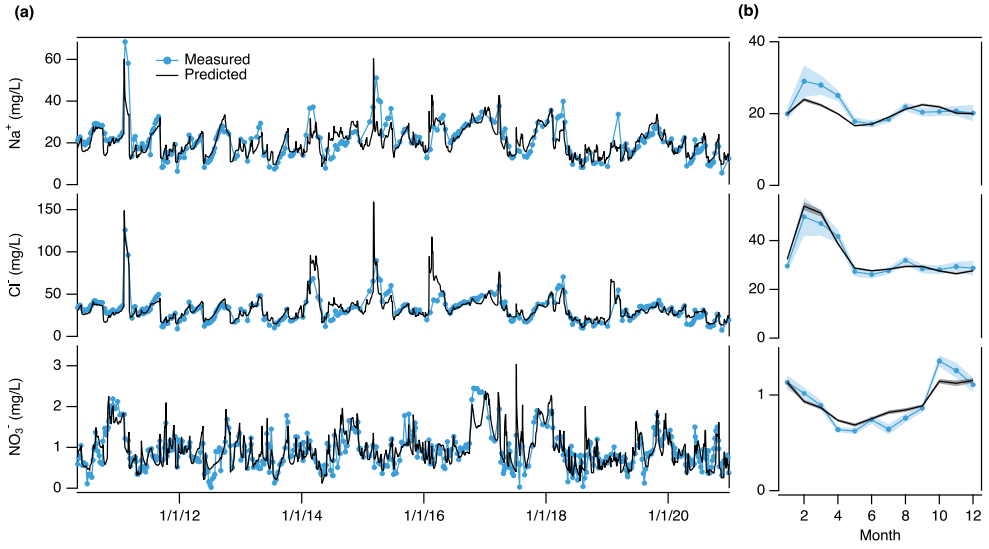

Fig. 8. (**a**) Weekly measured (blue circles) and daily model predicted (solid black curves) Na^+ (top panel), Cl^- (middle panel), and NO_3^- (bottom panel) concentrations near the Griffith drinking water treatment plant intake (ST01 in Fig. 1). Shaded bands represent estimates of model error. (**b**) Monthly average values of weekly measured (blue markers) model predicted (black curves) Na^+ (top panel), Cl^- (middle panel), and NO_3^- (bottom panel) concentrations near the Griffith drinking water intake. Shaded bands represent standard error of the mean.

4.4.4. Transit time model predictions at the base of the reservoir

The top-ranked models for Na^+, Cl^- and NO_3^- closely track measured concentrations of these three constituents at the base of the reservoir (Fig. 8a). The corresponding models for these three constituents utilize the same SAS functions for upstream (Shifted-Uniform) and distributed (Uniform) sources but differ with respect to the kinetic model employed (Null Kinetic Model for Na^+ and Cl^-, Non-Stationary Kinetic Model for NO_3^-) and the inferred scaling of Occoquan River concentrations for ungauged/groundwater source inflows (a = 0.97, 0.63, and 0.28 for Na^+, Cl^-, and NO_3^-, respectively). These top-ranked models perform remarkably well given their simplicity, relying on just two parameters for Na^+ and Cl^- and four parameters for NO_3^- (see performance metrics in Table 2).

The seasonal patterns of measured and predicted Na^+ and Cl^- concentrations at ST01 closely mirror those of upstream-source inflow concentrations (compare top two panels of Figs. 6b and 8b), consistent with the conservative nature of these two constituents in the reservoir. By contrast, inflow and outflow NO_3^- concentrations exhibit inverse seasonal patterns (higher summertime inflow concentrations but lower summertime outflow concentrations, compare bottom panels of Figs. 6b and 8b) reflecting enhanced nitrate removal via denitrification during periods of reservoir stratification (Fig. 7a).

5. Discussion

In this section, we discuss how the unsteady transit time theory described here can support water quality management in complex One Water systems, and explore its broader applications as well as possible technical challenges.

5.1. Water quality management in one water systems

5.1.1. Source attribution and management interventions

A key advantage of unsteady transit time theory is its parsimony and strong physical basis, which together support transparent analysis of how individual sources contribute to observed contaminant levels at the drinking water intake. To illustrate the model's utility for guiding intervention strategies and to gain mechanistic insight into seasonal patterns of Na^+, Cl^-, and NO_3^-, we conducted a sensitivity analysis in

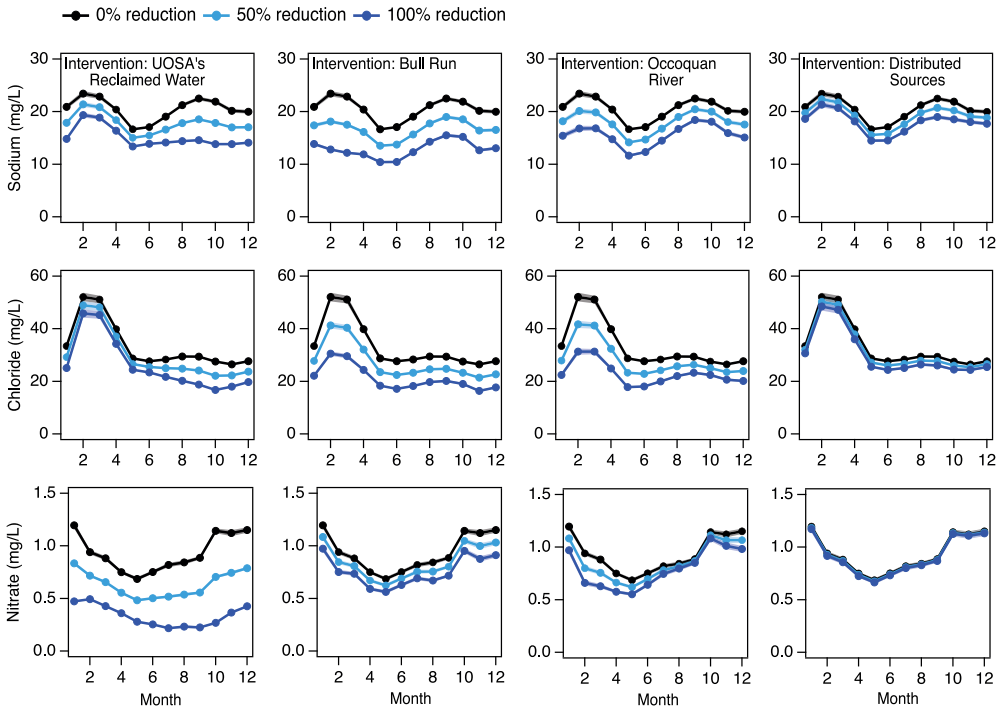

Fig. 9. Simulated effects of source-specific interventions on monthly average concentrations of Na^+, Cl^-, and NO_3^- at the base of the Occoquan Reservoir near the drinking water intake. Each column shows results for a different inflow – including UOSA's reclaimed water, Bull Run, Occoquan River, and distributed sources – under scenarios where the inflow concentrations from that source were reduced by 0% (black), 50% (light blue), and 100% (dark blue), while all other model inputs were held constant. Results are based on daily simulations over the 11-year study period (2010–2021) using the top-ranked unsteady transit time models (see Table 2). The daily predictions ($N = 4018$) were averaged monthly to yield the seasonal patterns presented here.

which inflow concentrations in upstream sources (UOSA's reclaimed water, Bull Run, and the Occoquan River) as well as in distributed sources (surface water and groundwater entering the reservoir along its perimeter, along with wet precipitation on the reservoir surface) were independently reduced by 0%, 50%, and 100%, while concentrations from all other sources were unchanged. For each intervention scenario, we simulated daily solute concentrations at the base of the reservoir over the 11-year study period and summarized the results as monthly averages (Fig. 9).

Three key insights emerge. First, reductions in distributed source concentrations have a negligible effect on solute concentrations at the drinking water intake. This outcome reflects both the relatively low volumetric contribution of distributed sources to the reservoir's water balance (≈22% on average) and their generally low concentrations compared to upstream sources ($a < 1$, see Table 2). Second, reducing concentrations in UOSA's reclaimed water leads to marked reductions in summertime Na^+ and Cl^- concentrations, effectively eliminating the summer peak in Na^+ that we previously attributed to diminished dilution of reclaimed water with watershed runoff during the summer. Reclaimed water also exerts strong control over NO_3^- concentrations, with reductions in NO_3^- loading from this source lowering concentrations of this nutrient throughout the year. Finally, the winter peaks in Na^+ and Cl^-, linked to deicer wash-off, are most sensitive to concentration reductions in outflow from the Bull Run and Occoquan River. These results affirm the dominant role of UOSA's reclaimed water in shaping summer-time chemistry at the drinking water intake, and urban runoff from the Bull Run and the Occoquan River watersheds in driving winter pulses of Na^+ and Cl^-. They also demonstrate the potential of this modeling framework to support targeted, source-specific management of salinization and nutrient loading (Grant et al., 2025).

5.1.2. Comparison to spatially resolved reservoir models

Because unsteady transit time theory is grounded in control volume analysis (i.e., it is a lumped model), it avoids the need to explicitly track internal water and solute movements within the reservoir. This structural simplicity allows for rigorous evaluation of alternative model structures (BIC ranking), rigorous statistical approaches for parameter inference (Bayesian MCMC), and rapid deployment for scenario testing (Fig. 9), and real-time interactive simulations (see next section). The unsteady transit time framework is also highly parsimonious, requiring only two fitted parameters for Na^+ and Cl^- and four for NO_3^- (Table 2), supporting robust parameter inference and scenario exploration.

By contrast, spatially resolved process-based modeling tools such as CE-QUAL-W2 or Delft3D require detailed bathymetry and segmentation, meteorological and heat flux data, hydrodynamic calibration (including turbulence/dispersion), and numerous water-quality rate coefficients and boundary conditions before they can be used to simulate reactive solute transport through a reservoir (Bai et al., 2022). In our experience at the Occoquan, graduate students required roughly a year to configure and calibrate a single CE-QUAL-W2 solution (Xu et al., 2007; Lodhi et al., 2019); by comparison, the unsteady transit time modeling framework presented here runs directly on measured reservoir inflows and outflows and can simulate decades of daily water quality at the drinking water intake in extraordinarily short run times (e.g., under 10 s on a standard laptop)—something that would be impractical with more complex spatially resolved models.

The trade-off for this parsimony and computational speed is that the transit time model cannot explicitly resolve within-reservoir circulation patterns or spatially resolved physicochemical processes that may influence the fate of some contaminants. For example, nitrate removal in the Occoquan Reservoir occurs primarily via denitrification in the hypolimnion during summer when the reservoir is stratified (Randall and Grizzard, 1995). While such stratification and depth-dependent reaction cannot be represented mechanistically within the transit time framework, they were successfully approximated here by allowing the transit-time–dependent reaction rate constant for denitrification to vary seasonally (e.g., higher during summer stratification, lower when the reservoir is mixed; Fig. 7). Other processes, such as turbulence-driven

exchange between the water column and sediments (Grant et al., 2020) and hyporheic exchange (Grant et al., 2020; Monofy et al., 2024), may be less amenable to representation in the transit time modeling framework. Systematic evaluation of conditions under which the unsteady transit time framework and spatially resolved models perform best remains an important area for future research.

5.1.3. Interactive scenario testing and participatory modeling

The low computational cost of the unsteady transit time model makes it well suited for simulating water quality outcomes under alternative management scenarios in real time (Gray et al., 2017), allowing stakeholders to explore trade-offs by adjusting source-specific inflow concentrations and immediately observe the predicted outcomes of their choices, along the lines of Fig. 9. As part of a U.S. National Science Foundation funded Growing Convergence Research project, we are using this approach to support stakeholder-driven solutions to cascading water quality challenges in the Occoquan Reservoir, including rising sodium ion concentrations (Bhide et al., 2021; Grant et al., 2022, 2025). More generally, unsteady transit time theory provides a transferable foundation for modeling and managing source-specific contaminant dynamics in One Water systems, offering a scalable pathway for integrating community and stakeholder input into coordinated, cross-sector responses to cascading water quality challenges.

5.2. Broader applications and technical insights

5.2.1. Shifted-uniform SAS function for upstream sources, $\Omega_1(S_t)$

To represent upstream source transport through the reservoir, we evaluated five different SAS functional forms, of which the Shifted-Uniform SAS emerged as the best choice based on model parsimony.

The Shifted-Uniform SAS function is a hydrologically unsteady analog of the tanks-in-series models commonly used in chemical engineering for reactor design (Hill, 2014). This SAS function splits upstream-source water and contaminants in storage into two tanks arranged in series (Grant and Harman, 2022) (Appendix D.1; Figure D.1). The upstream tank, which is assigned a plug-flow SAS, represents the advective transport of upstream-source water and solutes through the reservoir. The downstream tank, which is assigned a uniform SAS, represents dispersive mixing of upstream-source water and solutes as they transit through the reservoir. The SAS function's only parameter, p, represents the fraction of upstream source storage volume assigned to the upstream and downstream tanks, and thus the relative importance of advective versus dispersive mixing in the reservoir. The inferred value of the Shifted-Uniform SAS function parameter, $p = 0.51 \pm 0.003$, suggest that both down-reservoir advection (as modeled by the plug-flow component of the Shifted Uniform SAS) and dispersive mixing (as modeled by the uniform component) play an important role in the transport of upstream sources through the reservoir (Grant and Harman, 2022; Harman, 2015; Benettin et al., 2022).

5.2.2. Uniform SAS function for distributed sources, $\Omega_2(S_t)$

Distributed-source water and contaminant transport through the reservoir was represented here by a uniform SAS function—a choice justified by the diffuse nature of distributed inputs, which enter the reservoir all along its length and give rise to a broad distribution of transit times. The uniform SAS function, which samples water for outflow evenly from all ages in storage, provides a natural and parsimonious representation of this spatially distributed inflow behavior. An important benefit of this assumption is that it enables an immediate solution of the water balance for upstream and distributed sources, yielding explicit expressions for their respective contributions to reservoir storage and outflow (see Eqs. (7a)–(9b)). While alternative SAS functions might more accurately capture the influence of distributed sources on outlet water quality, our choice of a Uniform SAS is unlikely to bias results in the Occoquan Reservoir, where distributed sources contribute less inflow volume and contaminant mass, compared to upstream-sources. In systems where distributed sources are more dominant, the appropriateness of a uniform SAS may need to be reevaluated.

5.2.3. Extensibility to other environmental systems

While our implementation of unsteady transit time theory is framed around upstream and distributed source inflows to the Occoquan Reservoir, the underlying approach is broadly applicable to any system where solutes enter along distinct flow paths with different transit time distributions and source concentrations. This generalization of conventional unsteady transit time theory represents a key methodological advance: it extends unsteady transit time theory beyond idealized, single-source catchments to more complex and realistic environmental systems in which multiple sources contribute to observed water quality at a shared outlet. The strength of the approach lies in its flexibility, as transit time models can be independently applied to each source and then combined to simulate total concentration dynamics.

However, this extension comes with an important caveat: a mixing model must be introduced to account for how solutes from different sources combine at the outlet. In our study, the task was relatively straightforward, as the volumetric contributions of upstream and distributed inflows were separately estimated, enabling their mixing to be resolved via simple mass balance. In general, however, outlet mixing can be complex and uncertain (Liao et al., 2025). For example, Westfall et al. (2025) recently identified and evaluated 15 alternative mixing models for observed concentration–discharge relationships in 23 Australian streams. While outlet mixing remains a source of uncertainty and future research, the ability to represent source-specific dynamics using unsteady transit time theory represents a significant advance for environmental water quality modeling.

6. Conclusions

- This study extends unsteady transit time theory to settings with dual pollution sources, where a water body receives inputs both from upstream and from distributed sources along its perimeter.
- Applied to the Occoquan Reservoir, a drinking water supply for nearly one million people in Northern Virginia, the approach reproduced more than a decade of sodium, chloride, and nitrate measurements at the drinking water plant intake using only a handful of interpretable parameters.
- By avoiding the need to resolve detailed flow and transport within the reservoir, transit time theory simplifies model development and enables real-time simulations to support collaborative decision making.
- The framework is likely transferable to other drinking water contaminants and, more broadly, to cases where pollution enters a receiving water from multiple sources.

CRediT authorship contribution statement

Shantanu V. Bhide: Writing – review & editing, Writing – original draft, Visualization, Validation, Methodology, Formal analysis, Data curation, Conceptualization. **Stanley B. Grant:** Writing – review & editing, Writing – original draft, Supervision, Project administration, Methodology, Funding acquisition, Formal analysis, Conceptualization. **Paolo Benettin:** Writing – review & editing, Writing – original draft, Methodology, Conceptualization. **Megan A. Rippy:** Writing – review & editing, Funding acquisition, Formal analysis. **Ahmed Monofy:** Writing – review & editing, Formal analysis. **Kirin E. Furst:** Writing – review & editing. **Sydney Shelton:** Writing – review & editing. **Sujay S. Kaushal:** Writing – review & editing, Funding acquisition. **Shalini Misra:** Writing – review & editing, Project administration, Funding acquisition. **Peter J. Vikesland:** Writing – review & editing, Funding acquisition. **Erin R. Hotchkiss:** Writing – review & editing, Funding acquisition. **Anne Spiesman:** Writing – review & editing, Resources, Conceptualization. **Greg Prelewicz:** Resources. **Todd Schenk:** Writing – review & editing, Funding acquisition. **Harold Post:** Writing – original draft, Data curation. **Dongemei Alvi:** Writing – original draft, Data curation. **Brian Steglitz:** Writing – review & editing, Resources. **Admin Husic:** Writing – review & editing.

Declaration of competing interest

The authors declare that they have no known competing financial interests or personal relationships that could have appeared to influence the work reported in this paper.

Acknowledgments

The authors thank Shannon Curtis from Fairfax County and Brian Owsenek from Upper Occoquan Service Authority for valuable feedback on the manuscript. This research was supported with funding from a National Science Foundation (NSF), United States Growing Convergence Research grant (# 2021015, 2020814, and 2312326) and a NSF Civic Innovation Challenge grant (# 2431213). Additional support was provided by the Metropolitan Washington Council of Governments (MWCOG #21-001), Virginia Tech's College of Engineering H2OStorm Initiative, and the Northern Virginia Regional Commission.

Appendix A. Supplementary data

Supplementary material related to this article can be found online at https://doi.org/10.1016/j.watres.2025.124652.

Data availability

Data will be made available on request.

References

Appling, A.P., Leon, M.C., McDowell, W.H., 2015. Reducing bias and quantifying uncertainty in watershed flux estimates: the R package loadflex. Ecosphere 6 (12), 1–25. http://dx.doi.org/10.1890/ES14-00517.1, URL: https://onlinelibrary.wiley.com/doi/abs/10.1890/ES14-00517.1.

Assembly, V.G., 1971. Virginia Administrative Code - Title 9. Environment - Agency 25. State Water Control Board - Chapter 410. Occoquan Policy. URL: https://law.lis.virginia.gov/admincode/title9/agency25/chapter410/.

Bai, J., Zhao, J., Zhang, Z., Tian, Z., 2022. Assessment and a review of research on surface water quality modeling. Ecol. Model. 466, 109888. http://dx.doi.org/10.1016/j.ecolmodel.2022.109888, URL: https://linkinghub.elsevier.com/retrieve/pii/S0304380022000151.

Benettin, P., Kirchner, J.W., Rinaldo, A., Botter, G., 2015. Modeling chloride transport using travel time distributions at Plynlimon, Wales. Water Resour. Res. 51 (5), 3259–3276. http://dx.doi.org/10.1002/2014WR016600, URL: https://onlinelibrary.wiley.com/doi/abs/10.1002/2014WR016600. _eprint: https://onlinelibrary.wiley.com/doi/pdf/10.1002/2014WR016600.

Benettin, P., Queloz, P., Bensimon, M., McDonnell, J.J., Rinaldo, A., 2019. Velocities, Residence Times, Tracer Breakthroughs in a Vegetated Lysimeter: A Multitracer Experiment. Water Resour. Res. 55 (1), 21–33. http://dx.doi.org/10.1029/2018WR023894, URL: https://agupubs.onlinelibrary.wiley.com/doi/10.1029/2018WR023894.

Benettin, P., Rodriguez, N.B., Sprenger, M., Kim, M., Klaus, J., Harman, C.J., van der Velde, Y., Hrachowitz, M., Botter, G., McGuire, K.J., Kirchner, J.W., Rinaldo, A., McDonnell, J.J., 2022. Transit Time Estimation in Catchments: Recent Developments and Future Directions. Water Resour. Res. 58 (11), http://dx.doi.org/10.1029/2022WR033096, e2022WR033096. URL: https://onlinelibrary.wiley.com/doi/abs/10.1029/2022WR033096. _eprint: https://onlinelibrary.wiley.com/doi/pdf/10.1029/2022WR033096.

Bhide, S.V., Grant, S.B., Parker, E.A., Rippy, M.A., Godrej, A.N., Kaushal, S., Prelewicz, G., Saji, N., Curtis, S., Vikesland, P., Maile-Moskowitz, A., Edwards, M., Lopez, K.G., Birkland, T.A., Schenk, T., 2021. Addressing the contribution of indirect potable reuse to inland freshwater salinization. Nat. Sustain. 4 (8), 699–707. http://dx.doi.org/10.1038/s41893-021-00713-7, URL: https://www.nature.com/articles/s41893-021-00713-7.

Brewer, M.J., Butler, A., Cooksley, S.L., 2016. The relative performance of AIC, AIC_C and BIC in the presence of unobserved heterogeneity. In: Freckleton, R. (Ed.), Methods Ecol. Evol. 7 (6), 679–692. http://dx.doi.org/10.1111/2041-210X.12541, URL: https://besjournals.onlinelibrary.wiley.com/doi/10.1111/2041-210X.12541.

Conrad-Rooney, E., Gewirtzman, J., Pappas, Y., Pasquarella, V.J., Hutyra, L.R., Templer, P.H., 2023. Atmospheric wet deposition in urban and suburban sites across the United States. Atmos. Environ. 305, 119783. http://dx.doi.org/10.1016/j.atmosenv.2023.119783, URL: https://linkinghub.elsevier.com/retrieve/pii/S1352231023002091.

Costa, C.M.D.S.B., Leite, I.R., Almeida, A.K., De Almeida, I.K., 2021. Choosing an appropriate water quality model—a review. Environ. Monit. Assess. 193 (1), 38. http://dx.doi.org/10.1007/s10661-020-08786-1, URL: http://link.springer.com/10.1007/s10661-020-08786-1.

Crona, B.I., Parker, J.N., 2012. Learning in Support of Governance: Theories, Methods, and a Framework to Assess How Bridging Organizations Contribute to Adaptive Resource Governance. Ecol. Soc. 17 (1), URL: https://www.jstor.org/stable/26269019. Publisher: Resilience Alliance Inc..

Dewitz, J., 2020. National Land Cover Database (NLCD) 2016 Products (ver. 3.0, November 2023). http://dx.doi.org/10.5066/P96HHBIE, URL: https://www.sciencebase.gov/catalog/item/5d4c6a1de4b01d82ce8dfd2f.

Dombrowsky, I., Lenschow, A., Meergans, F., Schütze, N., Lukat, E., Stein, U., Yousefi, A., 2022. Effects of policy and functional (in)coherence on coordination – a comparative analysis of cross-sectoral water management problems. Environ. Sci. & Policy 131, 118–127. http://dx.doi.org/10.1016/j.envsci.2022.01.019, URL: https://www.sciencedirect.com/science/article/pii/S1462901122000302.

Environmental Protection Agency, 2024. PFAS National Primary Drinking Water Regulation. URL: https://www.federalregister.gov/documents/2024/04/26/2024-07773/pfas-national-primary-drinking-water-regulation,

Global Commission on the Economics of Water, 2024. The Economics of Water: Valuing the Hydrological Cycle as a Global Common Good. Technical Report, Global Commission on the Economics of Water, URL: https://economicsofwater.watercommission.org/.

Grant, S., Bhide, S., Spiesman, A., Misra, S., Rippy, M., Galik, C., Birkland, T., Schenk, T., Kaushal, S., Vikesland, P., Knocke, W., Husic, A., Post, H., Coneway, C., Prelewicz, G., Steglitz, B., Laursen, B., Rowles, K., Curtis, S., Studholme, A., 2025. Collaborative Solutions to Inland Freshwater Salinization. http://dx.doi.org/10.21203/rs.3.rs-6676897/v1, URL: https://www.researchsquare.com/article/rs-6676897/v1.

Grant, S.B., Gomez-Velez, J.D., Ghisalberti, M., Guymer, I., Boano, F., Roche, K., Harvey, J., 2020. A One-Dimensional Model for Turbulent Mixing in the Benthic Biolayer of Stream and Coastal Sediments. Water Resour. Res. 56 (12), http://dx.doi.org/10.1029/2019WR026822, e2019WR026822. URL: https://agupubs.onlinelibrary.wiley.com/doi/10.1029/2019WR026822.

Grant, S.B., Harman, C.J., 2022. Solute Transport Through Unsteady Hydrologic Systems Along a Plug Flow-To-Uniform Sampling Continuum. Water Resour. Res. 58 (8), http://dx.doi.org/10.1029/2022WR032038, e2022WR032038. URL: https://onlinelibrary.wiley.com/doi/abs/10.1029/2022WR032038.

Grant, S.B., Rippy, M.A., Birkland, T.A., Schenk, T., Rowles, K., Misra, S., Aminpour, P., Kaushal, S., Vikesland, P., Berglund, E., Gomez-Velez, J.D., Hotchkiss, E.R., Perez, G., Zhang, H.X., Armstrong, K., Bhide, S.V., Krauss, L., Maas, C., Mendoza, K., Shipman, C., Zhang, Y., Zhong, Y., 2022. Can Common Pool Resource Theory Catalyze Stakeholder-Driven Solutions to the Freshwater Salinization Syndrome? Environ. Sci. Technol. 56 (19), 13517–13527. http://dx.doi.org/10.1021/acs.est.2c01555.

Grant, S.B., Saphores, J.D., Feldman, D.L., Hamilton, A.J., Fletcher, T.D., Cook, P.L.M., Stewardson, M., Sanders, B.F., Levin, L.A., Ambrose, R.F., Deletic, A., Brown, R., Jiang, S.C., Rosso, D., Cooper, W.J., Marusic, I., 2012. Taking the "Waste" Out of "Wastewater" for Human Water Security and Ecosystem Sustainability. Science 337 (6095), 681–686. http://dx.doi.org/10.1126/science.1216852, Publisher: American Association for the Advancement of Science (AAAS).

Gray, S., Voinov, A., Paolisso, M., Jordan, R., BenDor, T., Bommel, P., Glynn, P., Hedelin, B., Hubacek, K., Introne, J., Kolagani, N., Laursen, B., Prell, C., Schmitt Olabisi, L., Singer, A., Sterling, E., Zellner, M., 2017. Purpose, processes, partnerships, and products: four Ps to advance participatory socio-environmental modeling. Ecol. Appl. 28 (1), 46–61. http://dx.doi.org/10.1002/eap.1627, URL: https://onlinelibrary.wiley.com/doi/abs/10.1002/eap.1627. _eprint: https://onlinelibrary.wiley.com/doi/pdf/10.1002/eap.1627.

Harman, C.J., 2015. Time-variable transit time distributions and transport: Theory and application to storage-dependent transport of chloride in a watershed. Water Resour. Res. 51 (1), 1–30. http://dx.doi.org/10.1002/2014WR015707, URL: https://onlinelibrary.wiley.com/doi/abs/10.1002/2014WR015707.

Harman, C.J., Ward, A.S., Ball, A., 2016. How does reach-scale stream-hyporheic transport vary with discharge? Insights from rSAS analysis of sequential tracer injections in a headwater mountain stream. Water Resour. Res. 52 (9), 7130–7150. http://dx.doi.org/10.1002/2016WR018832, URL: https://agupubs.onlinelibrary.wiley.com/doi/10.1002/2016WR018832.

Harman, C.J., Xu Fei, E., 2024. Mesas.py v1.0: a flexible Python package for modeling solute transport and transit times using StorAge Selection functions. Geosci. Model. Dev. 17 (2), 477–495. http://dx.doi.org/10.5194/gmd-17-477-2024, URL: https://gmd.copernicus.org/articles/17/477/2024/. Publisher: Copernicus GmbH.

Heasley, C., Sanchez, J.J., Tustin, J., Young, I., 2021. Systematic review of predictive models of microbial water quality at freshwater recreational beaches. In: Yaseen, Z.M. (Ed.), PLoS One 16 (8), e0256785. http://dx.doi.org/10.1371/journal.pone.0256785, URL: https://dx.plos.org/10.1371/journal.pone.0256785.

Hill, C.G., 2014. Introduction to Chemical Engineering Kinetics and Reactor Design, first ed. In: New York Academy of Sciences Series, John Wiley & Sons, Incorporated, Newark.

Hrachowitz, M., Benettin, P., van Breukelen, B.M., Fovet, O., Howden, N.J., Ruiz, L., van der Velde, Y., Wade, A.J., 2016. Transit times—the link between hydrology and water quality at the catchment scale. WIREs Water 3 (5), 629–657. http://dx.doi.org/10.1002/wat2.1155, URL: https://onlinelibrary.wiley.com/doi/abs/10.1002/wat2.1155.

Kaandorp, V.P., De Louw, P.G.B., Van Der Velde, Y., Broers, H.P., 2018. Transient Groundwater Travel Time Distributions and Age-Ranked Storage-Discharge Relationships of Three Lowland Catchments. Water Resour. Res. 54 (7), 4519–4536. http://dx.doi.org/10.1029/2017WR022461, URL: https://agupubs.onlinelibrary.wiley.com/doi/10.1029/2017WR022461.

Kaushal, S.S., Likens, G.E., Mayer, P.M., Shatkay, R.R., Shelton, S.A., Grant, S.B., Utz, R.M., Yaculak, A.M., Maas, C.M., Reimer, J.E., Bhide, S.V., Malin, J.T., Rippy, M.A., 2023. The anthropogenic salt cycle. Nat. Rev. Earth & Environ. 4 (11), 770–784. http://dx.doi.org/10.1038/s43017-023-00485-y, URL: https://www.nature.com/articles/s43017-023-00485-y. Number: 11 Publisher: Nature Publishing Group.

Kim, M., Pangle, L.A., Cardoso, C., Lora, M., Volkmann, T.H.M., Wang, Y., Harman, C.J., Troch, P.A., 2016. Transit time distributions and StorAge Selection functions in a sloping soil lysimeter with time-varying flow paths: Direct observation of internal and external transport variability. Water Resour. Res. 52 (9), 7105–7129. http://dx.doi.org/10.1002/2016WR018620, URL: https://onlinelibrary.wiley.com/doi/abs/10.1002/2016WR018620. _eprint: https://onlinelibrary.wiley.com/doi/pdf/10.1002/2016WR018620.

King, H., 1918. Handbook of Hydraulics for the Solution of Hydraulic Problems. McGraw-Hill book Company, Incorporated, URL: https://books.google.com/books?id=F8Y3AAAAMAAJ.

Kiparsky, M., Thompson, B.H., Binz, C., Sedlak, D.L., Tummers, L., Truffer, B., 2016. Barriers to Innovation in Urban Wastewater Utilities: Attitudes of Managers in California. Environ. Manag. 57 (6), 1204–1216. http://dx.doi.org/10.1007/s00267-016-0685-3.

Kirchner, J.W., Feng, X., Neal, C., 2000. Fractal stream chemistry and its implications for contaminant transport in catchments. Nature 403 (6769), 524–527. http://dx.doi.org/10.1038/35000537, URL: https://www.nature.com/articles/35000537.

Koban, L.A., King, T., Huff, T.B., Furst, K.E., Nelson, T.R., Pfluger, A.R., Kuppa, M.M., Fowler, A.E., 2024. Passive biomonitoring for per- and polyfluoroalkyl substances using invasive clams, c. fluminea. J. Hazard. Mater. 472, 134463. http://dx.doi.org/10.1016/j.jhazmat.2024.134463, URL: https://linkinghub.elsevier.com/retrieve/pii/S0304389424010422.

Liao, A., Zhou, T., Song, X., Yang, L., Han, D., Yang, S., 2025. Understanding Flow Transport in Dual-Water-Source Rivers: Enhancing Storage Selection Functions With Two-Gamma Distributions. Hydrol. Process. 39 (4), e70121. http://dx.doi.org/10.1002/hyp.70121, URL: https://onlinelibrary.wiley.com/doi/10.1002/hyp.70121.

Lindenschmidt, K.-E., Carr, M.K., Sadeghian, A., Morales-Marin, L., 2019. CE-QUAL-W2 model of dam outflow elevation impact on temperature, dissolved oxygen and nutrients in a reservoir. Sci. Data 6 (1), 312. http://dx.doi.org/10.1038/s41597-019-0316-y, URL: https://www.nature.com/articles/s41597-019-0316-y.

Liu, L., Lopez, E., Dueñas-Osorio, L., Stadler, L., Xie, Y., Alvarez, P.J.J., Li, Q., 2020. The importance of system configuration for distributed direct potable water reuse. Nat. Sustain. 3 (7), 548–555. http://dx.doi.org/10.1038/s41893-020-0518-5, URL: https://www.nature.com/articles/s41893-020-0518-5. Number: 7 Publisher: Nature Publishing Group.

Lodhi, A.G., Godrej, A.N., Sen, D., Angelotti, R., Brooks, M., 2019. A decision support system for indirect potable reuse based on integrated modeling and futurecasting. J. Water Reuse Desalination 9 (3), 263–281. http://dx.doi.org/10.2166/wrd.2019.071, URL: https://iwaponline.com/jwrd/article/9/3/263/66790/A-decision-support-system-for-indirect-potable.

Margerum, R.D., 2011. Beyond Consensus: Improving Collaborative Planning and Management. MIT Press, Google-Books-ID: gNLxCwAAQBAJ.

Masoumi, F., Afshar, A., Palatkaleh, S.T., 2016. Selective withdrawal optimization in river–reservoir systems; trade-offs between maximum allowable receiving waste load and water quality criteria enhancement. Environ. Monit. Assess. 188 (7), 390. http://dx.doi.org/10.1007/s10661-016-5386-0, URL: http://link.springer.com/10.1007/s10661-016-5386-0.

McGuire, K.J., McDonnell, J.J., 2006. A review and evaluation of catchment transit time modeling. J. Hydrol. 330 (3), 543–563. http://dx.doi.org/10.1016/j.jhydrol.2006.04.020, URL: https://www.sciencedirect.com/science/article/pii/S0022169406002150.

Miles, P., 2019. Pymcmcstat: A Python Package for Bayesian Inference Using Delayed Rejection Adaptive Metropolis. J. Open Source Softw. 4 (38), 1417. http://dx.doi.org/10.21105/joss.01417, URL: http://joss.theoj.org/papers/10.21105/joss.01417.

Monofy, A., Grant, S.B., Boano, F., Rippy, M.A., Gomez-Velez, J.D., Kaushal, S.S., Hotchkiss, E.R., Shelton, S., 2024. Toward a Universal Model of Hyporheic Exchange and Nutrient Cycling in Streams. AGU Adv. 5 (6), http://dx.doi.org/10.1029/2024AV001373, e2024AV001373. URL: https://agupubs.onlinelibrary.wiley.com/doi/10.1029/2024AV001373.

Mukheibir, P., Howe, C., Gallet, D., 2014. What's getting in the way of a "one water" approach to water services planning and management? Water: J. Aust. Water Assoc. 41 (3), 67–73, URL: https://search.informit.org/doi/10.3316/informit.612935719954220. Place: St Leonards, NSW, Australia Publisher: Australian Water Association.

Mulholland, P.J., Helton, A.M., Poole, G.C., Hall, R.O., Hamilton, S.K., Peterson, B.J., Tank, J.L., Ashkenas, L.R., Cooper, L.W., Dahm, C.N., Dodds, W.K., Findlay, S.E.G., Gregory, S.V., Grimm, N.B., Johnson, S.L., McDowell, W.H., Meyer, J.L., Valett, H.M., Webster, J.R., Arango, C.P., Beaulieu, J.J., Bernot, M.J., Burgin, A.J., Crenshaw, C.L., Johnson, L.T., Niederlehner, B.R., O'Brien, J.M., Potter, J.D., Sheibley, R.W., Sobota, D.J., Thomas, S.M., 2008. Stream denitrification across biomes and its response to anthropogenic nitrate loading. Nature 452 (7184), 202–205. http://dx.doi.org/10.1038/nature06686, URL: https://www.nature.com/articles/nature06686.

Nagel, B., Partelow, S., 2022. A methodological guide for applying the social-ecological system (SES) framework: a review of quantitative approaches. Ecol. Soc. 27 (4), http://dx.doi.org/10.5751/ES-13493-270439, URL: https://ecologyandsociety.org/vol27/iss4/art39/. Publisher: The Resilience Alliance.

Ostrom, E., 2009. A General Framework for Analyzing Sustainability of Social-Ecological Systems. Science 325 (5939), 419–422. http://dx.doi.org/10.1126/science.1172133, URL: https://www.science.org/doi/full/10.1126/science.1172133?casa_token=ycTEhnj56QIAAAAA%3AVw05Fbj_aBHRHki3emzWpuBzzHtlGJnRI_s2k8VUIeF7fBUsyDouWzlr47KfYBAraEKesbivcXml.

Palacin-Lizarbe, C., Camarero, L., Catalan, J., 2018. Denitrification Temperature Dependence in Remote, Cold, and N-Poor Lake Sediments. Water Resour. Res. 54 (2), 1161–1173. http://dx.doi.org/10.1002/2017WR021680, URL: https://agupubs.onlinelibrary.wiley.com/doi/10.1002/2017WR021680.

Pandit, A., Golden, H., Christensen, J., Lane, C.R., Husic, A., 2025. Deep learning prediction and interpretation of riverine nitrate export across the Mississippi River Basin (In Revision). Water Resour. Res..

Parker, E.A., Grant, S.B., Sahin, A., Vrugt, J.A., Brand, M.W., 2022. Can Smart Stormwater Systems Outsmart the Weather? Stormwater Capture with Real-Time Control in Southern California. ACS ES&T Water 2 (1), 10–21. http://dx.doi.org/10.1021/acsestwater.1c00173.

Piña-Ochoa, E., Álvarez-Cobelas, M., 2006. Denitrification in Aquatic Environments: A Cross-system Analysis. Biogeochemistry 81 (1), 111–130. http://dx.doi.org/10.1007/s10533-006-9033-7, URL: http://link.springer.com/10.1007/s10533-006-9033-7.

Pokhrel, S.R., Chhipi-Shrestha, G., Hewage, K., Sadiq, R., 2022. Sustainable, resilient, and reliable urban water systems: making the case for a "one water" approach. Environ. Rev. 30 (1), 10–29. http://dx.doi.org/10.1139/er-2020-0090, URL: https://cdnsciencepub.com/doi/full/10.1139/er-2020-0090. Publisher: NRC Research Press.

Rahaman, M.M., Varis, O., 2005. Integrated water resources management: evolution, prospects and future challenges. Sustain.: Sci. Pr. Policy 1 (1), 15–21. http://dx.doi.org/10.1080/15487733.2005.11907961, URL: https://www.tandfonline.com/doi/full/10.1080/15487733.2005.11907961.

Randall, C.W., Grizzard, T.J., 1995. Management of the occoquan river basin: A 20-year case history. River Basin Management for Sustainable Development, Water Sci. Technol. River Basin Management for Sustainable Development, 32 (5), 235–243. http://dx.doi.org/10.1016/0273-1223(95)00668-0.URL: https://www.sciencedirect.com/science/article/pii/0273122395006680,

Rinaldo, A., Beven, K.J., Bertuzzo, E., Nicotina, L., Davies, J., Fiori, A., Russo, D., Botter, G., 2011. Catchment travel time distributions and water flow in soils. Water Resour. Res. 47 (7), http://dx.doi.org/10.1029/2011WR010478, 2011WR010478. URL: https://agupubs.onlinelibrary.wiley.com/doi/10.1029/2011WR010478.

Rippy, M., Roston, B., Berglund, E., Aminpour, P., Krauss, L., Bhide, S., Schenk, T., Rowles, K., Misra, S., Birkland, T., Kaushal, S., Grant, S., 2024. Characterizing the social-ecological system for inland freshwater salinization using fuzzy cognitive maps: implications for collective management. Ecol. Soc. 29 (4), art47. http://dx.doi.org/10.5751/ES-15536-290447, URL: https://www.ecologyandsociety.org/vol29/iss4/art47/.

Roa-García, M.C., Weiler, M., 2010. Integrated response and transit time distributions of watersheds by combining hydrograph separation and long-term transit time modeling. Hydrol. Earth Syst. Sci. 14 (8), 1537–1549. http://dx.doi.org/10.5194/hess-14-1537-2010, URL: https://hess.copernicus.org/articles/14/1537/2010/.

Seitzinger, S., Harrison, J.A., Böhlke, J.K., Bouwman, A.F., Lowrance, R., Peterson, B., Tobias, C., Drecht, G.V., 2006. Denitrification Across Landscapes and Waterscapes: A Synthesis. Ecol. Appl. 16 (6), 2064–2090. http://dx.doi.org/10.1890/1051-0761(2006)016[2064:DALAWA]2.0.CO;2, URL: http://doi.wiley.com/10.1890/1051-0761(2006)016[2064:DALAWA]2.0.CO;2.

Smith, A.A., Tetzlaff, D., Soulsby, C., 2018. On the Use of StorAge Selection Functions to Assess Time-Variant Travel Times in Lakes. Water Resour. Res. 54 (7), 5163–5185. http://dx.doi.org/10.1029/2017WR021242, URL:

https://onlinelibrary.wiley.com/doi/abs/10.1029/2017WR021242. _eprint: https://onlinelibrary.wiley.com/doi/pdf/10.1029/2017WR021242.

Steel, B.S., Lach, D., Weber, E.P., 2017. New Strategies for Wicked Problems: Science and Solutions in the 21st Century. Oregon State University Press, Corvallis, http://dx.doi.org/10.1353/book56396.

Weglarczyk, S.a., 1998. The interdependence and applicability of some statistical quality measures for hydrological models. J. Hydrol. 206 (1–2), 98–103. http://dx.doi.org/10.1016/S0022-1694(98)00094-8, URL: https://linkinghub.elsevier.com/retrieve/pii/S0022169498000948.

Westfall, T.G., Peterson, T.J., Lintern, A., Western, A.W., 2025. Slow and Quick Flow Models Explain the Temporal Dynamics of Daily Salinity in Streams. Water Resour. Res. 61 (6), http://dx.doi.org/10.1029/2024WR039103, e2024WR039103. URL: https://agupubs.onlinelibrary.wiley.com/doi/10.1029/2024WR039103.

Xu, Z., Godrej, A.N., Grizzard, T.J., 2007. The hydrological calibration and validation of a complexly-linked watershed–reservoir model for the Occoquan watershed, Virginia. J. Hydrol. 345 (3–4), 167–183. http://dx.doi.org/10.1016/j.jhydrol.2007.07.015, URL: https://linkinghub.elsevier.com/retrieve/pii/S0022169407004325.